

15

Spur Gears

15.1 Introduction and History

Gears, defined as toothed members transmitting rotary motion from one shaft to another, are among the oldest devices and inventions of man. In about 2600 B.C., the Chinese are known to have used a chariot incorporating a complex series of gears like those illustrated in Figure 15.1. Aristotle, in the fourth century B.C., wrote of gears as though they were commonplace. In the fifteenth century A.D., Leonardo da Vinci designed a multitude of devices incorporating many kinds of gears.

Among the various means of mechanical power transmission (including primarily gears, belts, and chains), gears are generally the most rugged and durable. Their power transmission efficiency is as high as 98%. On the other hand, gears are usually more costly than chains and belts. As would be expected, gear manufacturing costs increase sharply with increased precision—as required for the combination of high speeds and heavy loads, and for low noise levels. (Standard tolerances for various degrees of manufacturing precision have been established by the AGMA, American Gear Manufacturers Association.)

Spur gears are the simplest and most common type of gears. As shown in Figure 15.2, they are used to transfer motion between parallel shafts, and they have teeth that are parallel to the shaft axes. The major portion of our study of spur gears will be concerned with gear geometry and nomenclature (Sections 15.2 and 15.3), gear force analysis (Section 15.4), gear-tooth bending strength (Sections 15.6 through 15.8), and gear-tooth surface durability (Sections 15.9 and 15.10).

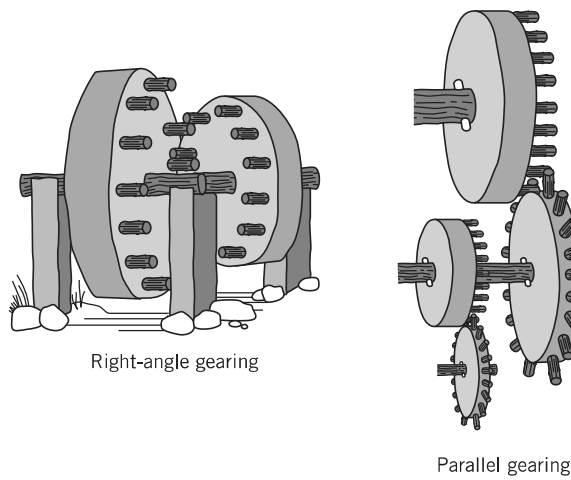


FIGURE 15.1 Primitive gears.

The engineer seriously involved with gears of any kind should consult the pertinent standards of the AGMA, as well as other contemporary gear literature. The site <http://www.machinedesign.com> presents general information on gear drives, gear tooth forms, and gearboxes. The site <http://www.powertransmission.com> provides websites for manufacturers of gears and gear drives.

15.2 Geometry and Nomenclature

The basic requirement of gear-tooth geometry is the provision of angular velocity ratios that are exactly constant. For example, the angular-velocity ratio between a 20-tooth and a 40-tooth gear must be precisely 2 in every position. It must not be, for example, 1.99 as a given pair of teeth come into mesh and then 2.01 as they go out of mesh. Of course, manufacturing inaccuracies and tooth deflections will cause slight deviations in velocity ratio, but acceptable tooth profiles are based on theoretical curves that meet this criterion.

The action of a pair of gear teeth satisfying this requirement is termed *conjugate gear-tooth action*, and is illustrated in Figure 15.3. The basic law of conjugate gear-tooth action states that

As the gears rotate, the common normal to the surfaces at the point of contact must always intersect the line of centers at the same point P, called the pitch point.

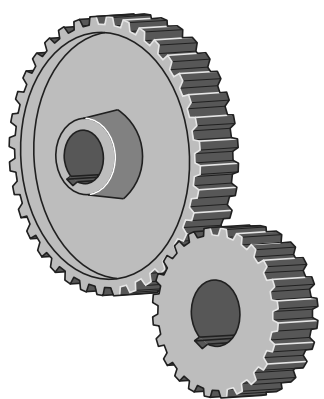


FIGURE 15.2 Spur gears.

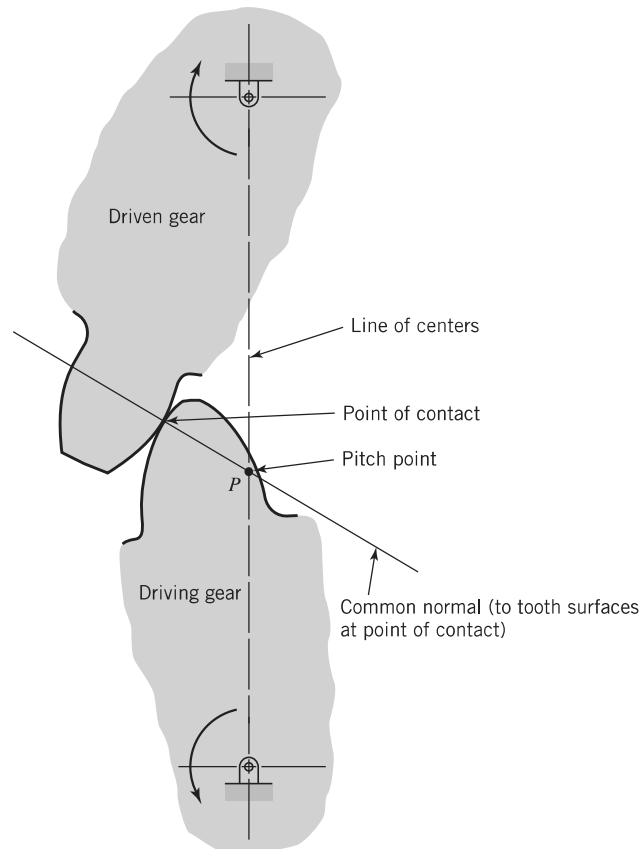


FIGURE 15.3 Conjugate gear-tooth action.

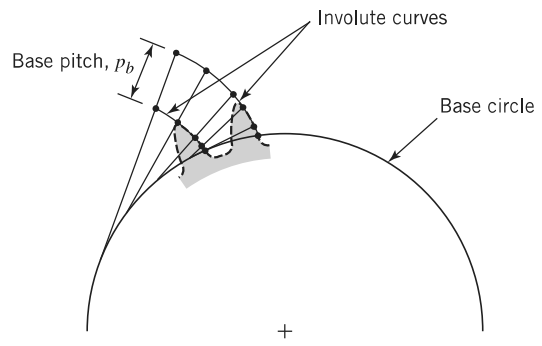


FIGURE 15.4 Generation of an involute from its base circle.

The law of conjugate gear-tooth action can be satisfied by various tooth shapes, but the only one of current importance is the *involute*, or, more precisely, the *involute of the circle*. An involute (of the circle) is the curve generated by any point on a taut thread as it unwinds from a circle, called the *base circle*. The generation of two involutes is shown in Figure 15.4. The dotted lines show how these could correspond to the outer portions of the right sides of adjacent gear teeth. Correspondingly, involutes generated by unwinding a thread wrapped counterclockwise around the base circle would form the outer portions of the left sides of the teeth. Note that at every point, the involute is perpendicular to the taut thread. It is important to note that an involute can be developed as far as desired *outside* the base circle, but *an involute cannot exist inside its base circle*.

An understanding of a mating pair of involute gear teeth can be developed from a study of (1) a friction drive, (2) a belt drive, and, finally, (3) an involute gear-tooth drive. Figure 15.5 shows two *pitch circles*. Imagine that they represent two cylinders pressed together. If there is no slippage, rotation of one cylinder (pitch circle) will cause rotation of the other at an angular-velocity ratio inversely proportional to their diameters. In any pair of mating gears, the smaller of the two is called the *pinion* and the larger one the *gear*. The term “*gear*” is used in a general sense to indicate either of the members and also in a specific sense to indicate the larger of the two. A bit confusing, perhaps, but life is sometimes like that! Using subscripts *p* and *g* to denote pinion and gear, respectively, we have

$$\omega_p / \omega_g = -d_g / d_p \quad (15.1)$$

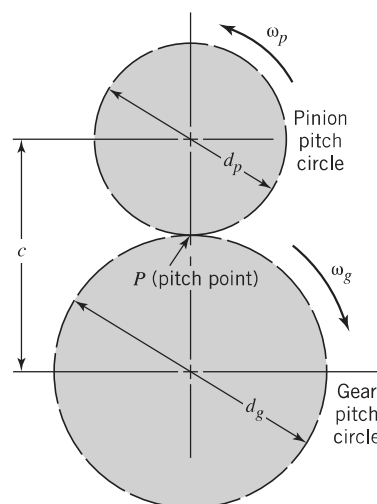


FIGURE 15.5 Friction gears of diameter d rotating at angular velocity ω .

where ω is the angular velocity, d is the pitch diameter, and the minus sign indicates that the two cylinders (gears) rotate in opposite directions. The *center distance* is

$$c = (d_p + d_g)/2 = r_p + r_g \quad (15.1a)$$

where r is the *pitch circle radius*.

In order to transmit more torque than is possible with friction gears alone, we now add a belt drive running between pulleys representing the *base circles*, as in Figure 15.6. If the pinion is turned counterclockwise a few degrees, the belt will cause the gear to rotate in accordance with Eq. 15.1. In gear parlance, angle ϕ is called the *pressure angle*. From similar triangles, the base circles have the same ratio as the pitch circles; thus, the velocity ratios provided by the friction and belt drives are the same.

In Figure 15.7, the belt is cut at point c , and the two ends are used to generate involute profiles de and fg for the pinion and gear, respectively. It should now be clear why ϕ is called the pressure angle: neglecting sliding friction, the force of one involute tooth pushing against the other is always at an angle equal to the pressure angle. A comparison of Figures 15.7 and 15.3

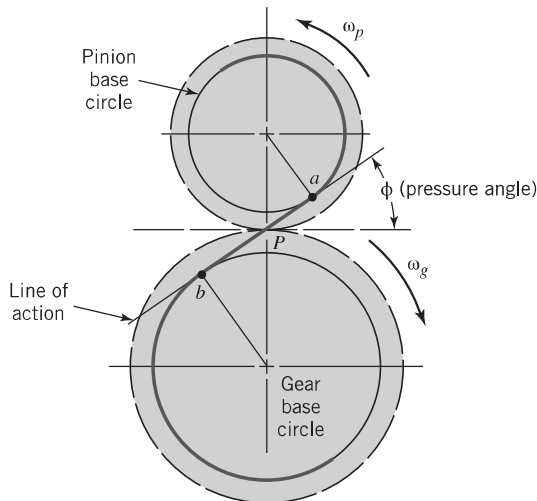


FIGURE 15.6 Belt drive added to friction gears.

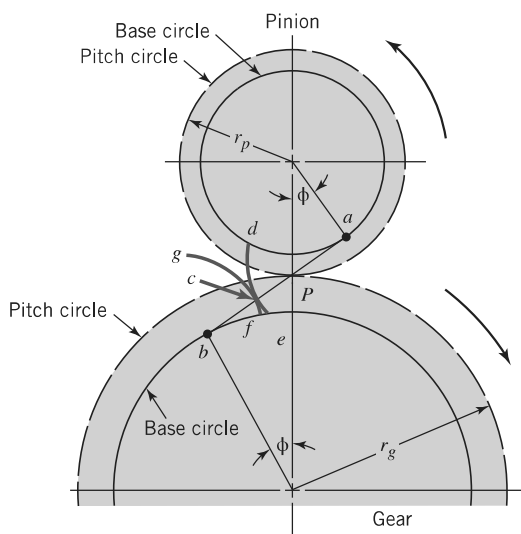


FIGURE 15.7 Belt cut at c to generate conjugate involute profiles.

shows that the involute profiles do indeed satisfy the fundamental law of conjugate gear-tooth action. Incidentally, the involute is the only geometric profile satisfying this law that maintains a constant-pressure angle as the gears rotate. Note especially that conjugate involute action can take place only outside of both base circles. In Figure 15.7, the conjugate involute profiles could be drawn only by “cutting the belt” at a point between a and b .

Figure 15.8 shows the continued development of the gear teeth. The involute profiles are extended outward beyond the pitch circle by a distance called the *addendum*. The outer circle is usually called the *addendum circle*. Similarly, the tooth profiles are extended inward from the pitch circle a distance called the *dedendum*. Of course, the involute portion can extend inward only to the base circle. The portion of the profile between the base and dedendum (root) circles cannot participate in the conjugate involute action but must clear the tip of a mating tooth as the gears rotate. This portion of the tooth profile is usually drawn as a straight radial line, but its actual shape (which depends on the manufacturing process) is usually trochoidal. A fillet at the

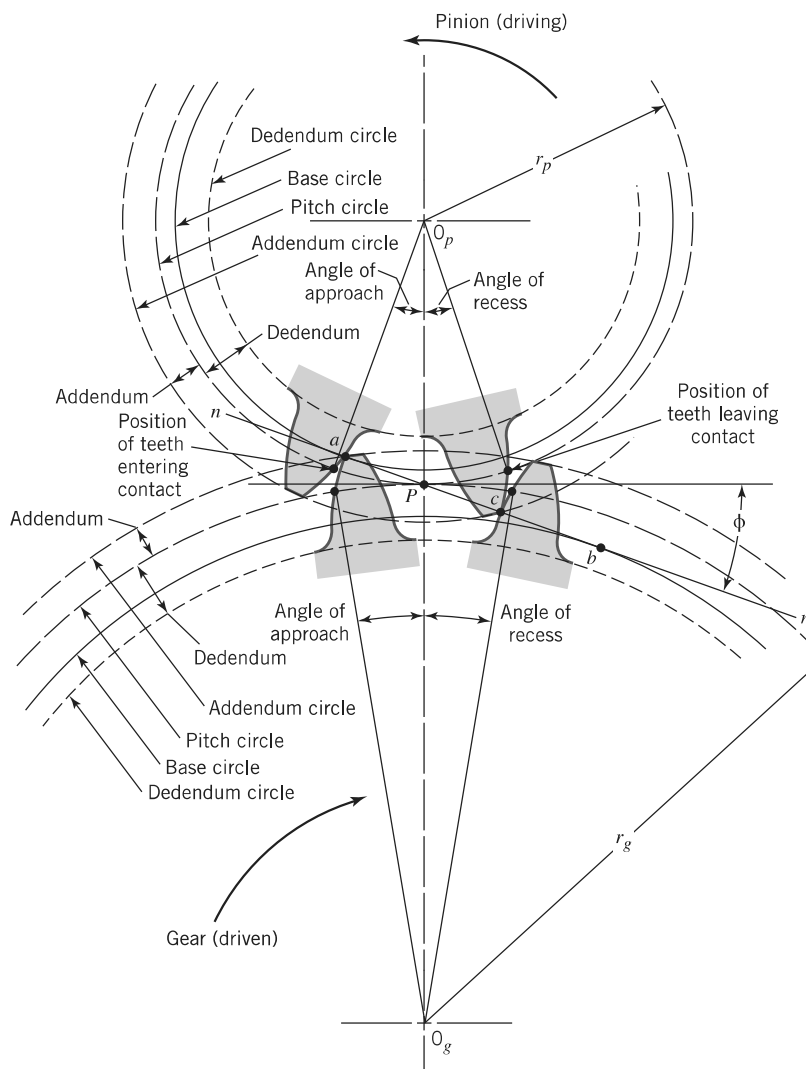


FIGURE 15.8 Further development and nomenclature of involute gear teeth. Note: The diagram shows the special case of maximum possible gear addendum without interference; pinion addendum is far short of the theoretical limit.

base of the tooth blends the profile into the dedendum (root) circle. This fillet is important to reduce bending stress concentration.

An important point to keep in mind is that the “diameter” (without a qualifying adjective) of a gear always refers to its *pitch diameter*. If other diameters (base, root, outside, etc.) are intended, they are always specified. Similarly, d , without subscripts, refers to *pitch diameter*. The pitch diameters of a pinion and gear are distinguished by subscripts p and g ; thus, d_p and d_g are their symbols.

Figure 15.8 shows the gear addendum extended exactly to point of tangency a . (The pinion addendum extends to arbitrary point c , which is short of tangency point b .) This gear addendum represents the theoretical maximum without encountering “interference,” which is discussed in the next section. Mating gears of standard proportions generally have shorter addenda (like the pinion in Figure 15.8). For practical reasons, the addenda of mating gears should not extend quite to the tangency points.

Figure 15.8 shows the position of a pair of mating teeth as they enter contact and again as they go out of contact. Note the corresponding *angle of approach* and *angle of recess* for both pinion and gear (measured to points on the pitch circles).

Line nn (Figure 15.8) is called the *line of action* (neglecting friction, the force between mating teeth always acts along this line). The *path of contact* (locus of all points of tooth contact) is a segment of this line. In Figure 15.8, the path of contact is the line segment ac .

Further nomenclature relating to the complete gear tooth is shown in Figure 15.9. Various terms associated with gears and gear assemblies are summarized in Appendix J. *Face* and *flank* portions of the tooth surface are divided by the *pitch cylinder* (which contains the pitch circle). Note in particular, the *circular pitch*, designated as p , and measured in inches (English units) or millimeters (SI units). If N is the number of teeth in the gear (or pinion) and d the pitch diameter, then

$$p = \frac{\pi d}{N}, \quad p = \frac{\pi d_p}{N_p}, \quad p = \frac{\pi d_g}{N_g} \quad (p \text{ in inches}) \quad (15.2)$$

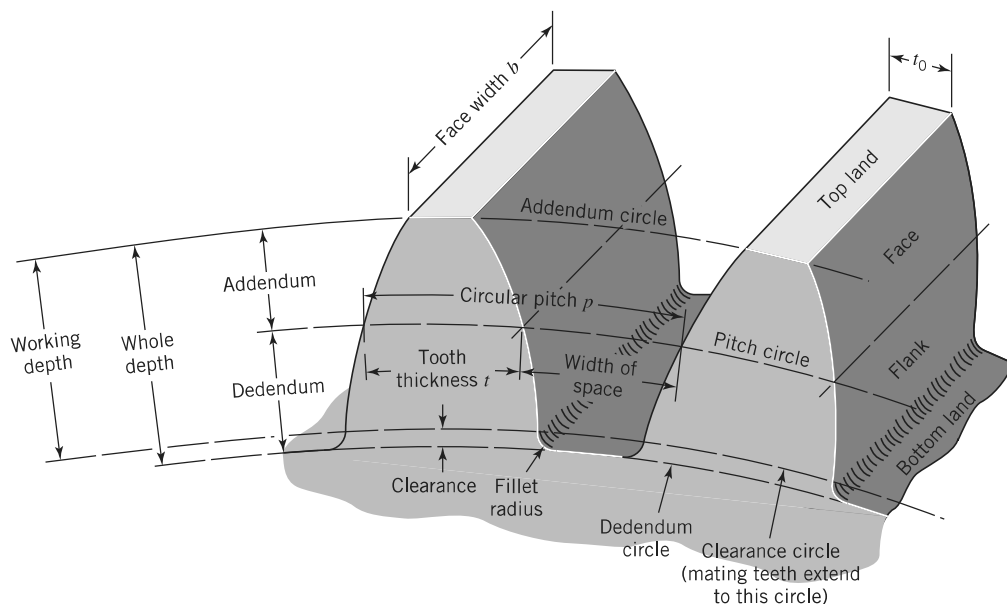


FIGURE 15.9 Nomenclature of gear teeth.

More commonly used indices of gear-tooth size and *diametral pitch* P (used *only* with English units) and *module m* (used *only* with SI or metric units). Diametral pitch is defined as the number of teeth per *inch* of pitch diameter:

$$P = \frac{N}{d}, \quad P = \frac{N_p}{d_p}, \quad P = \frac{N_g}{d_g} \quad (P \text{ in teeth per inch}) \quad (15.3)$$

Module m , which is essentially the reciprocal of P , is defined as the pitch diameter in *millimeters* divided by the number of teeth (number of millimeters of pitch diameter per tooth):

$$m = \frac{d}{N}, \quad m = \frac{d_p}{N_p}, \quad m = \frac{d_g}{N_g} \quad (m \text{ in millimeters per tooth}) \quad (15.4)$$

The reader can readily verify that

$$pP = \pi \quad (p \text{ in inches; } P \text{ in teeth per inch}) \quad (15.5)$$

$$p/m = \pi \quad (p \text{ in millimeters; } m \text{ in millimeters per tooth}) \quad (15.6)$$

$$m = 25.4/P \quad (15.7)$$

With English units, the word “pitch,” without a qualifying adjective, means *diametral* pitch (a “12-pitch gear” refers to a gear with 12 teeth per inch of pitch diameter), whereas with SI units, “pitch” means *circular* pitch (a “gear of pitch = 3.14 mm” refers to a gear having a circular pitch of 3.14 mm).

Gears are commonly made to an integral value of diametral pitch (English units) or standard value of module (SI units). Figure 15.10 shows the actual size of gear teeth of several standard

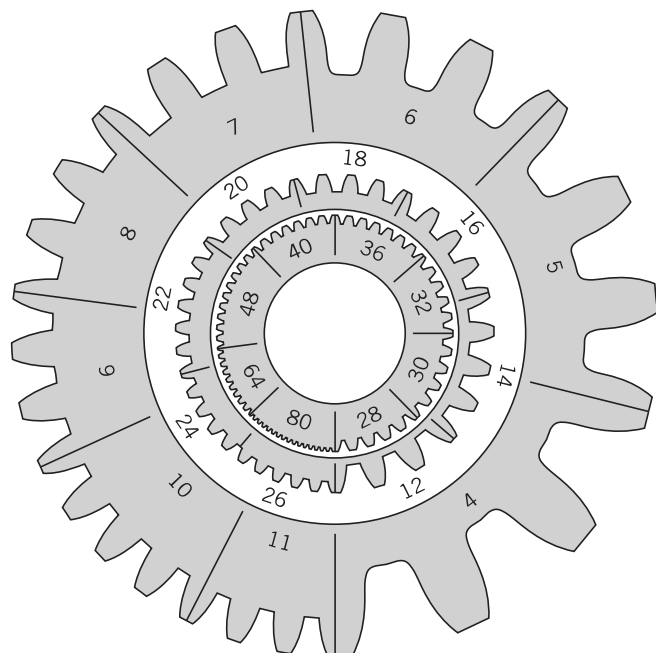


FIGURE 15.10 Actual sizes of gear teeth of various diametral pitches.
Note: In general, fine-pitch gears have $P \geq 20$; coarse-pitch gears have $P < 20$. (Bourn & Koch Machine Tool Company.)

diametral pitches. With SI units, commonly used standard values of module are

0.2 to 1.0 by increments of 0.1

1.0 to 4.0 by increments of 0.25

4.0 to 5.0 by increments of 0.5

The most commonly used pressure angle, ϕ , with both English and SI units is 20° . In the United States, 25° is also standard, and 14.5° was formerly an alternative standard value.

For all systems, the standard addendum is $1/P$ (in inches) or m (in millimeters), and the standard dedendum is 1.25 times the addendum.¹ A former standard system in the United States was the 20° stub system, for which the addendum was shortened to $0.8/P$. (Although 14.5° gears and 20° stub gears are no longer standard, replacement gears are still made for these systems.) The fillet radius (at the base of the tooth) is commonly about $0.35/P$ (English units) or $m/3$ (SI units).

Face width, b (defined in Figure 15.9), is not standardized, but generally,

$$\frac{9}{P} < b < \frac{14}{P} \quad (\text{a})$$

or

$$9m < b < 14m \quad (\text{b})$$

The wider the face width, the more difficult it is to manufacture and mount the gears so that contact is uniform across the full face width.

Gears made to standard systems are interchangeable and are usually available in stock. On the other hand, mass-produced gears used for particular applications (like automobile transmission gears) deviate from these standards in order to be optimal for their specific application. The present trend is toward greater use of special gears, for modern gear-cutting equipment reduces the cost penalty involved, and modern computer facilities minimize the engineering design time required.

Figure 15.11 shows a pinion in contact with a *rack*, which can be thought of as a segment of a gear of infinite diameter. Figure 15.12 shows a pinion in contact with an *internal gear*. The

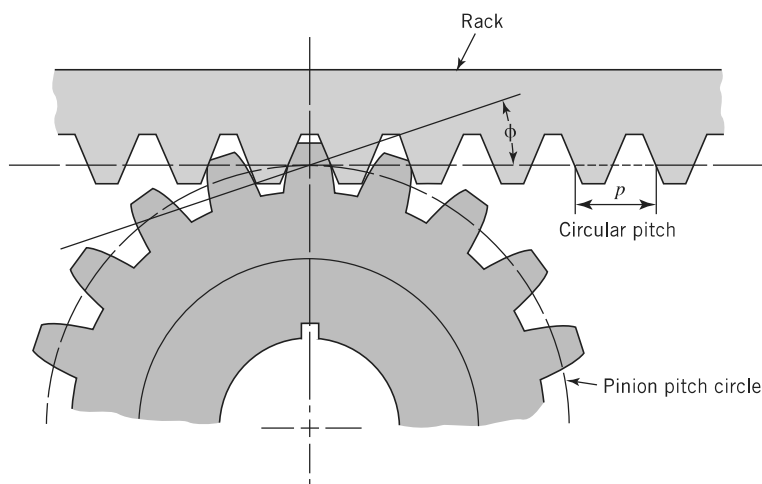


FIGURE 15.11 Involute pinion and rack.

¹For fine-pitch gears of $P \geq 20$, the standard dedendum is $(1.20/P) + 0.002$ in.

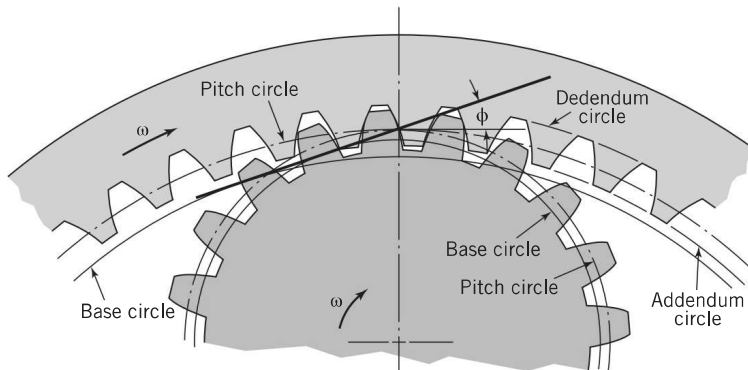


FIGURE 15.12 Involute pinion and internal gear. Note that both rotate in the same direction.

internal gear is also called an *annulus*, or *ring* gear, and is commonly used in the planetary gear trains of automotive automatic transmissions (see Section 15.13). Diameters of internal gears are considered *negative*; hence, Eq. 15.1 indicates that a pinion and internal gear rotate in the *same* direction.

An important advantage of the involute form over all others is that it provides theoretically perfect conjugate action even when the shaft center distances are not exactly correct. This fact can be verified by reviewing the basic development of involute profiles in Figures 15.6 and 15.7. If the shafts of two mating gears are separated, proper action continues with an increased pressure angle. Of course, the *backlash* (shortest distance between the noncontacting surfaces of adjacent teeth) increases as center distance is increased. In some cases, advantage is taken of this feature by adjusting the shaft center distance to obtain desired backlash. (Some backlash is necessary to allow room for an oil film under all conditions of thermal expansion and contraction, but excessive backlash increases noise and impact loading whenever torque reversals occur.)

A second basic advantage of the involute system is that the profile for the basic rack is a straight line. This facilitates cutter manufacture and gear-tooth generation.

The cutting of gear teeth is a highly developed engineering art and science. Two of the several methods used are shown in Figures 15.13 and 15.14.

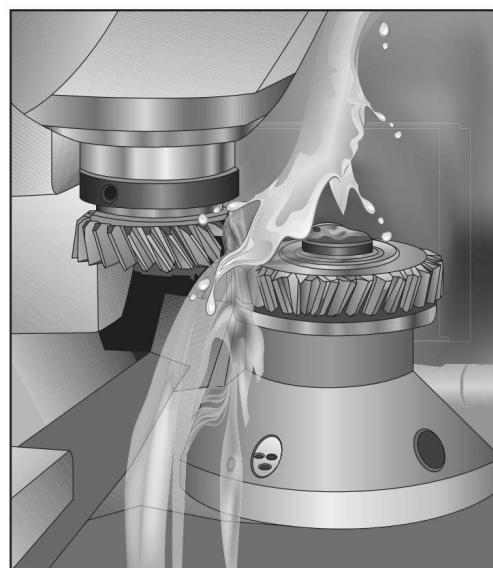


FIGURE 15.13 Generating a gear with a shaping machine suitable for external and internal gears.

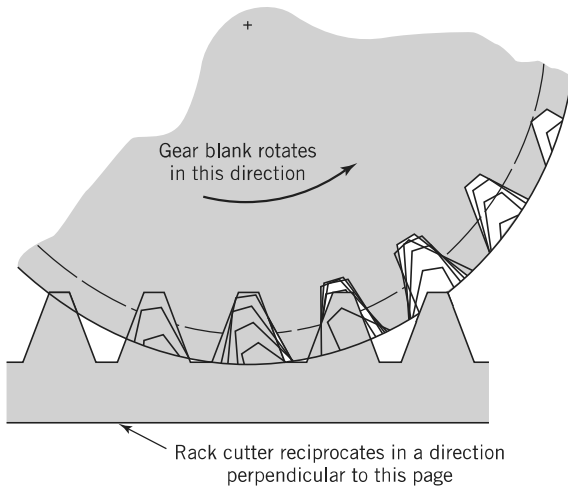


FIGURE 15.14 Shaping teeth with a rack cutter.

15.3 Interference and Contact Ratio

Interference will occur, preventing rotation of the mating gears, if either of the addendum circles extends beyond tangent points a and b (Figures 15.6 through 15.8), which are called *interference points*. In Figure 15.15, both addendum circles extend beyond the interference points; hence, these gears will not operate without modification. The preferred correction is to remove the interfering tooth tips, shown shaded. Alternatively, the tooth flanks of the mating gear can be undercut in order to clear the offending tips, but this weakens the teeth. In no case, is it possible to have useful contact of the shaded tips, as conjugate involute action is not possible beyond the interference points.

When teeth are generated with a rack cutter, as in Figure 15.14, the teeth are *automatically* undercut if they would interfere with a rack. This undercutting takes place with standard 20° pinions with fewer than 18 teeth, and with standard 25° pinions having fewer than 12 teeth. For this reason, pinions with fewer than these numbers of teeth are not normally used with standard tooth proportions.

From Figure 15.15 or 15.8,

$$r_a = r + a$$

where

r_a = addendum circle radius

r = pitch circle radius

a = addendum

We can also obtain the equation for the maximum possible addendum circle radius without interference,

$$r_{a(\max)} = \sqrt{r_b^2 + c^2 \sin^2 \phi} \quad (15.8)$$

where

$r_{a(\max)}$ = maximum noninterfering addendum circle radius of pinion or gear

r_b = base circle radius of the same member

c = center distance, O_1O_2

ϕ = pressure angle (*actual*, not nominal, value)

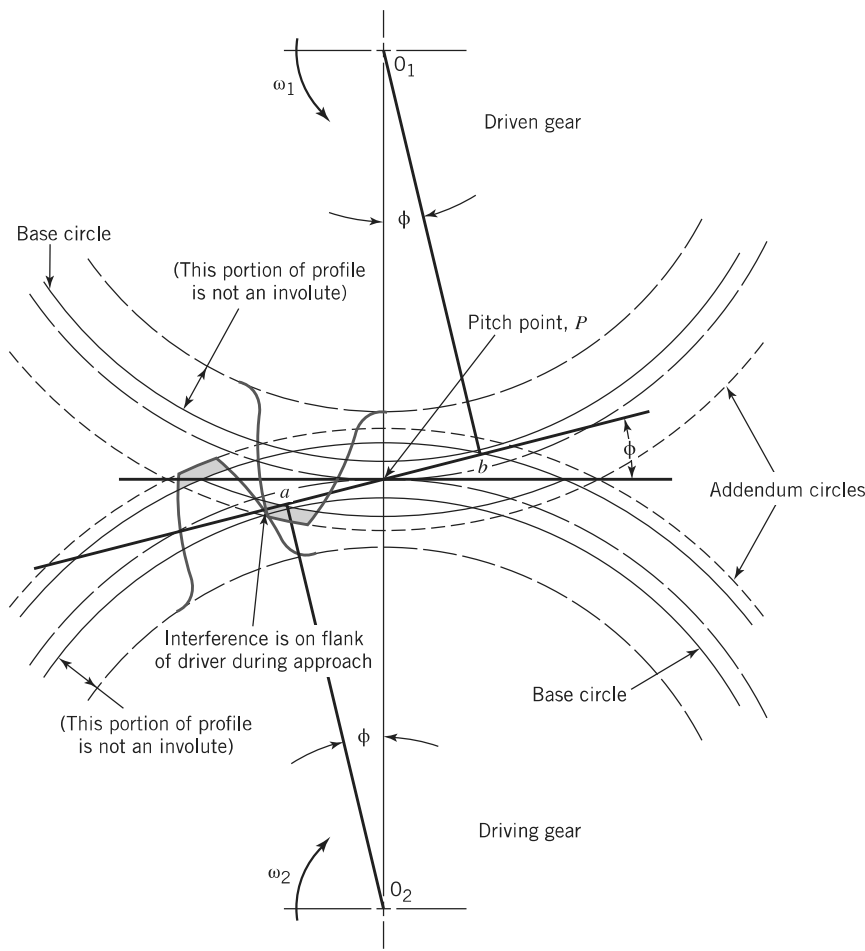


FIGURE 15.15 Interference of spur gears (eliminated by removing the shaded tooth tips).

A study of Eq. 15.8 and its derivation indicates that (1) interference is more likely to involve the tips of the gear teeth than the tips of the pinion teeth and (2) interference is promoted by having a *small* number of pinion teeth, a *large* number of gear teeth, and a *small* pressure angle.

It is obviously necessary that the tooth profiles be proportioned so that a second pair of mating teeth come into contact before the first pair is out of contact. The average number of teeth in contact as the gears rotate together is the *contact ratio* (CR), which is calculated from the following equation [1],

$$CR = \frac{\sqrt{r_{ap}^2 - r_{bp}^2} + \sqrt{r_{ag}^2 - r_{bg}^2} - c \sin \phi}{p_b} \quad (15.9)$$

where

$$\begin{aligned} r_{ap}, r_{ag} &= \text{addendum radii of the mating pinion and gear} \\ r_{bp}, r_{bg} &= \text{base circle radii of the mating pinion and gear} \end{aligned}$$

The *base pitch* p_b is

$$p_b = \pi d_b / N \quad (15.10)$$

where N = number of teeth and d_b = diameter of the base circle. From Figure 15.7

$$d_b = d \cos \phi, \quad r_b = r \cos \phi, \quad \text{and} \quad p_b = p \cos \phi \quad (15.11)$$

The base pitch is like the circular pitch except that it represents an arc of the base circle rather than an arc of the pitch circle. It is illustrated in Figure 15.4.

In general, the greater the contact ratio, the smoother and quieter the operation of the gears. A contact ratio of 2 or more means that at least two pairs of teeth are theoretically in contact at all times. (Whether or not they are *actually* in contact depends on the precision of manufacture, tooth stiffness, and applied load.)

An algorithmic approach to computing the contact ratio is described in Appendix J.

SAMPLE PROBLEM 15.1D Meshing Spur Gear and Pinion

Two parallel shafts with 4-in. center distance are to be connected by 6-pitch, 20° spur gears providing a velocity ratio of -3.0 . (a) Determine the pitch diameters and numbers of teeth in the pinion and gear. (b) Determine whether there will be interference when standard full-depth teeth are used. (c) Determine the contact ratio. (See Figure 15.16.)

SOLUTION

Known: Spur gears of known pitch size, pressure angle, and center distance mesh to provide a known velocity ratio.

Find:

- Determine pitch diameters (d_p, d_g) and the numbers of teeth (N_p, N_g).
- Determine the possibility of interference with standard full-depth teeth.
- Calculate the contact ratio (CR).

Schematic and Given Data:

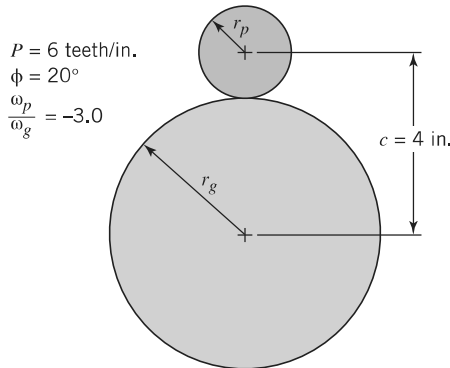


FIGURE 15.16 Spur gears for Sample Problem 15.1D.

Decisions and Assumptions:

- If interference results from the use of standard full-depth gear teeth, unequal addenda gears will be selected.
- The gear teeth will have standard involute tooth profiles.
- The two gears will be located at their theoretical center distance, $c = (d_p + d_g)/2$ where $d_p = N_p/P$, $d_g = N_g/P$; that is, the gears will mesh at their pitch circles.

Design Analysis:

1. We have $r_p + r_g = c = 4$ in.; $r_g/r_p = -\text{velocity ratio} = 3$; hence, $r_p = 1$ in., $r_g = 3$ in., or $d_p = 2$ in., $d_g = 6$ in.
2. The term “6-pitch gears” means that $P = 6$ teeth per inch of pitch diameter; hence, $N_p = 12$, $N_g = 36$.
3. In order to use Eq. 15.8 to check for interference, we first determine the base circle radii of pinion and gear. From Eq. 15.11, $r_{bp} = 1$ in. ($\cos 20^\circ$), and $r_{bg} = 3$ in. ($\cos 20^\circ$). Substitution in Eq. 15.8 gives $r_{a(\max)} = 1.660$ in. for the pinion and 3.133 in. for the gear.
4. The limiting outer gear radius is equivalent to an addendum of only 0.133 in., whereas a standard full-depth tooth has an addendum of $1/P = 0.167$ in. Clearly, the use of standard teeth would cause interference.
5. Let us use unequal addenda gears (nonstandard), with somewhat arbitrarily chosen addenda of $a_g = 0.060$ in. for the gear and $a_p = 0.290$ in. for the pinion. (The reasoning is to select maximum addenda for greatest contact ratio, while at the same time limiting the gear addendum to stay safely away from interference, and limiting the pinion addendum to maintain adequate width of top land. The latter is shown as t_0 in Figure 15.9, and its minimum acceptable value is sometimes taken as $0.25/P$.)
6. Substitution in Eq. 15.11 gives $p_b = (\pi/6) \cos 20^\circ = 0.492$ in. Substitution in Eq. 15.9 [with $r_{ap} = 1.290$ in., $r_{bp} = 1$ in. ($\cos 20^\circ$), $r_{ag} = 3.060$ in., $r_{bg} = 3$ in. ($\cos 20^\circ$)] gives CR = 1.43, which should be a suitable value.

Comments:

1. If after the gears are mounted, the center distance is found to be slightly greater than the theoretical (calculated) center distance of 4.0 in., this would mean that the calculated diameters, d_p and d_g , are smaller than the actual gear and pinion pitch diameters and that the backlash is greater than initially calculated.
2. Had we wished to use standard tooth proportions in solving this sample problem, we could have (a) increased the diametral pitch (thereby giving more teeth on the pinion—and this outweighs the influence of giving more teeth to the gear) or (b) increased the pressure angle to 25° (which would be more than enough to eliminate interference).
3. This problem may also be solved using the worksheet in Appendix J.

15.4 Gear Force Analysis

It was noted in Figures 15.7 and 15.8 that line *ab* was always normal to the contacting tooth surfaces and that (neglecting sliding friction) it was the *line of action* of the forces between mating teeth.

The force between mating teeth can be resolved at the pitch point (*P*, in Figures 15.15 and 15.17) into two components.

1. Tangential component F_t , which, when multiplied by the pitch line velocity, accounts for the power transmitted.
2. Radial component F_r , which does no work but tends to push the gears apart.

Figure 15.17 illustrates that the relationship between these components is

$$F_r = F_t \tan \phi \quad (15.12)$$

To analyze the relationships between the gear force components and the associated shaft power and rotating speed, we note that the gear pitch line velocity *V*, in feet per minute, is equal to

$$V = \pi d n / 12 \quad (15.13)$$

where *d* is the pitch diameter in inches of the gear rotating *n* rpm.

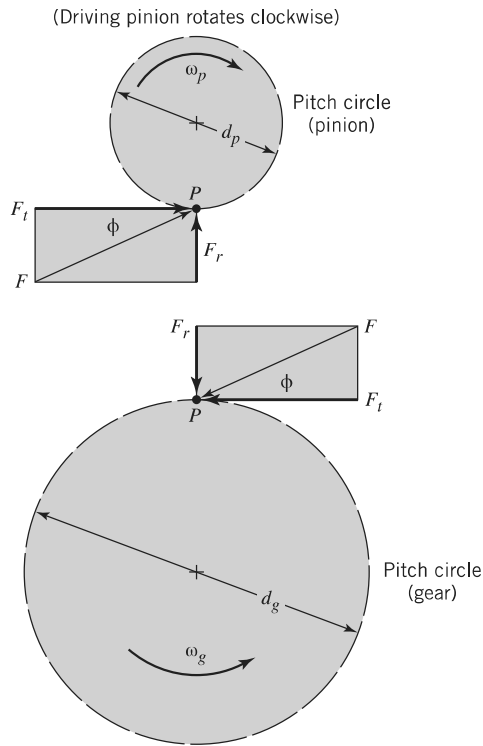


FIGURE 15.17 Gear-tooth force F , shown resolved at pitch point. The driving pinion and driven gear are shown separately.

The transmitted power in horsepower (hp) is

$$\dot{W} = F_t V / 33,000 \quad (15.14)$$

where F_t is in pounds and V is in feet per minute.

In SI units

$$V = \pi d n / 60,000 \quad (15.13a)$$

where d is in millimeters, n in rpm, and V in meters per second. Transmitted power in watts (W) is

$$\dot{W} = F_t V \quad (15.14a)$$

where F_t is in newtons.

SAMPLE PROBLEM 15.2 Forces on Spur Gears

Figure 15.18a shows three gears of $P = 3$, $\phi = 20^\circ$. Gear a is the driving, or input, pinion. It rotates counter-clockwise at 600 rpm and transmits 25 hp to idler gear b . Output gear c is attached to a shaft that drives a machine. Nothing is attached to the idler shaft, and friction losses in the bearings and gears can be neglected. Determine the resultant load applied by the idler to its shaft.

SOLUTION

Known: Three spur gears of specified diametral pitch, numbers of teeth, and pressure angle mesh to transmit 25 hp from input gear to output gear through an idler gear. The input gear rotation speed and direction are given.

Find: Determine the resultant load of the idler gear on its shaft.

Schematic and Given Data:

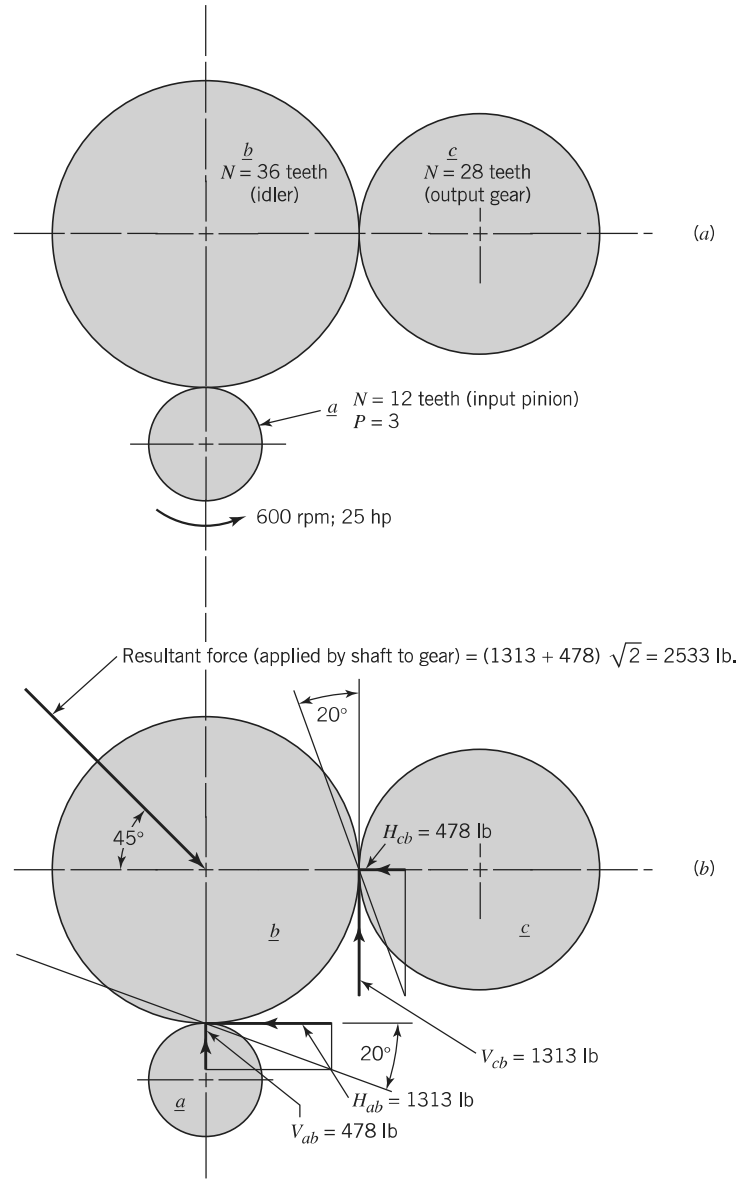


FIGURE 15.18 Gear forces in Sample Problem 15.2.
(a) Gear layout. (b) Forces acting on idler *b*.

Assumptions:

1. The idler gear and shaft serve the function of transmitting power from the input gear to the output gear.
No idler shaft torque is applied to the idler gear.
2. Friction losses in the bearings and gears are negligible.
3. The gears mesh at the pitch circles.
4. The gear teeth have standard involute tooth profiles.
5. The shafts for gears *a*, *b*, and *c* are parallel.

Analysis:

1. Applying Eq. 15.3 to gear *a* gives

$$d_a = N_a/P = (12 \text{ teeth})/(3 \text{ teeth per inch}) = 4 \text{ in.}$$

2. All three gears have the same pitch line velocity. Applying Eq. 15.13 to gear *a*, we have

$$V = \frac{\pi d_a n_a}{12} = \frac{\pi(4 \text{ in.})(600 \text{ rpm})}{12} = 628.28 \text{ ft/min}$$

3. Applying Eq. 15.14 to gear *a* and solving for F_t gives

$$F_t = \frac{33,000(25 \text{ hp})}{628.28 \text{ fpm}} = 1313 \text{ lb}$$

This is the horizontal force of gear *b* applied to gear *a*, directed to the right. Figure 15.18b shows the equal and opposite horizontal force of *a* applied to *b*, labeled H_{ab} , and acting to the left.

4. From Eq. 15.12, the corresponding radial gear-tooth force is $F_r = V_{ab} = (1313)(\tan 20^\circ) = 478 \text{ lb}$.
5. Forces H_{cb} and V_{cb} are shown in proper direction in Figure 15.18b. (Remember, these are forces applied by *c* to *b*.) Since the shaft supporting idler *b* carries no torque, equilibrium of moments about its axis of rotation requires that $V_{cb} = 1313 \text{ lb}$. From Eq. 15.12, $H_{cb} = (1313)(\tan 20^\circ)$, or 478 lb.
6. Total gear-tooth forces acting on *b* are $1313 + 478 = 1791 \text{ lb}$ both vertically and horizontally, for a vector sum of $1791 \sqrt{2} = 2533 \text{ lb}$ acting at 45° . This is the resultant load applied by the idler to its shaft.

Comment: The equal and opposite force applied by the shaft to the idler gear is shown in Figure 15.18b, where the idler is shown as a free body in equilibrium.

15.5 Gear-Tooth Strength

Having dealt with gear geometry and force analysis, we now turn to the question of how much power or torque a given pair of gears will transmit without tooth failure. Figure 15.19 shows a *photoelastic pattern* of gear-tooth stresses. The details of this experimental stress analysis procedure are beyond the scope of this book, and it is sufficient here to note that the highest stresses exist where the lines are bunched closest together. This occurs at two locations: (1) the point of contact with the mating gear, where force F is acting and (2) in the fillet at the base of the tooth.

The next three sections deal with bending fatigue at the base of the tooth and involve the principles of fatigue analysis covered in Chapter 8. The following two sections are concerned

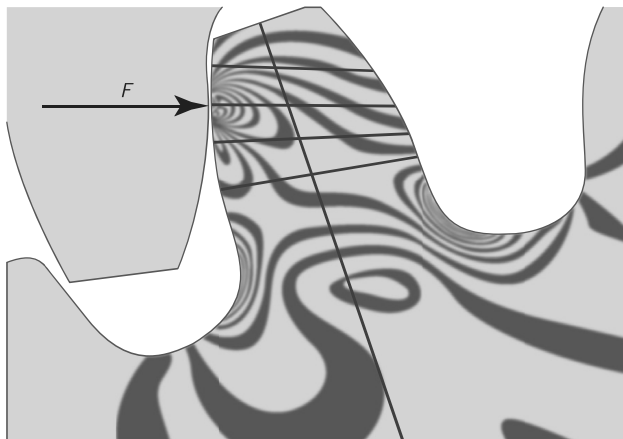


FIGURE 15.19 Photoelastic pattern of stresses in a spur gear tooth.

with surface durability and make use of the information on pitting and scoring given in Chapter 9. Some of the principles of lubrication covered in Chapter 13 are involved as well. As will be seen, the load capacity and failure mode of a pair of gears are affected by their rotating speed. Altogether, the study of gear load capacity affords an excellent opportunity to apply much of the basic material covered in earlier chapters.

15.6 Basic Analysis of Gear-Tooth-Bending Stress (Lewis Equation)

The first recognized analysis of gear-tooth stresses was presented to the Philadelphia Engineers Club in 1892 by Wilfred Lewis. It still serves as the basis for gear-tooth-bending stress analysis. Figure 15.20 shows a gear tooth loaded as a cantilever beam, with resultant force F applied to the tip. Mr. Lewis made the following simplifying assumptions:

1. *The full load is applied to the tip of a single tooth.* This is obviously the most severe condition and is appropriate for gears of “ordinary” accuracy. For high-precision gears, however, the full load is never applied to a single tooth tip. With a contact ratio necessarily greater than unity, each new pair of teeth comes into contact while the previous pair is still engaged. After the contact point moves down some distance from the tip, the previous teeth go out of engagement and the new pair carries the full load (unless, of course, the contact ratio is greater than 2). This is the situation depicted in Figure 15.19. Thus, with *precision gears* (not available in Mr. Lewis’s time), the tooth should be regarded as carrying only part of the load at its tip, and the full load at a point on the tooth face where the bending moment arm is shorter.
2. *The radial component, F_r , is negligible.* This is a conservative assumption, as F_r produces a compressive stress that subtracts from the bending tension at point a of Figure 15.20. (The fact that it adds to the bending compression in the opposite fillet is unimportant because fatigue failures always start on the tensile side.)
3. *The load is distributed uniformly across the full face width.* This is a nonconservative assumption and can be instrumental in gear failures involving wide teeth and misaligned or deflecting shafts.

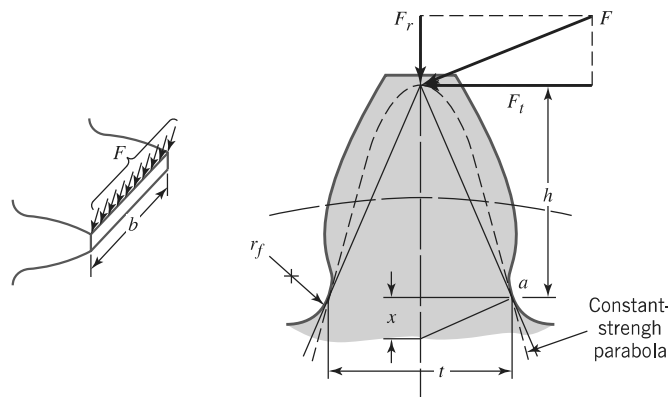


FIGURE 15.20 Bending stresses in a spur gear tooth (comparison with a constant-stress parabola).

4. Forces which are due to tooth sliding friction are negligible.
5. Stress concentration in the tooth fillet is negligible. Stress concentration factors were unknown in Mr. Lewis's time but are now known to be important. This will be taken into account later.

Proceeding with the development of the Lewis equation, we note from Figure 15.20 that the gear tooth is everywhere stronger than the inscribed *constant-strength parabola* (recall Figure 12.23c), except for the section at *a* where the parabola and tooth profile are tangent. At point *a*

$$\sigma = \frac{Mc}{I} = \frac{6F_t h}{bt^2} \quad (\text{c})$$

by similar triangles,

$$\frac{t/2}{x} = \frac{h}{t/2} \quad \text{or} \quad \frac{t^2}{h} = 4x \quad (\text{d})$$

Substituting Eq. d into Eq. c gives

$$\sigma = \frac{6F_t}{4bx} \quad (\text{e})$$

Defining the *Lewis form factor* *y* as

$$y = 2x/3p \quad (\text{f})$$

and substituting it into Eq. e gives

$$\sigma = \frac{F_t}{bpy} \quad (\text{15.15})$$

which is the basic *Lewis equation* in terms of circular pitch.

Because gears are more often made to standard values of diametral pitch, we substitute

$$p = \pi/P \quad (\text{15.5, mod})$$

$$y = Y/\pi \quad (\text{g})$$

into Eq. 15.14 and obtain an alternative form of the Lewis equation:

$$\sigma = \frac{F_t P}{bY} \quad (\text{15.16})$$

Or, when using SI units, we have

$$\sigma = \frac{F_t}{mbY} \quad (\text{15.16a})$$

where *Y* is the Lewis form factor based on diametral pitch or module. Both *Y* and *y* are functions of tooth *shape* (but not size) and therefore vary with the number of teeth in the gear. Values of *Y* for standard gear systems are given in Figure 15.21. For nonstandard gears, the factor can be obtained by graphical layout of the tooth or by digital computation.

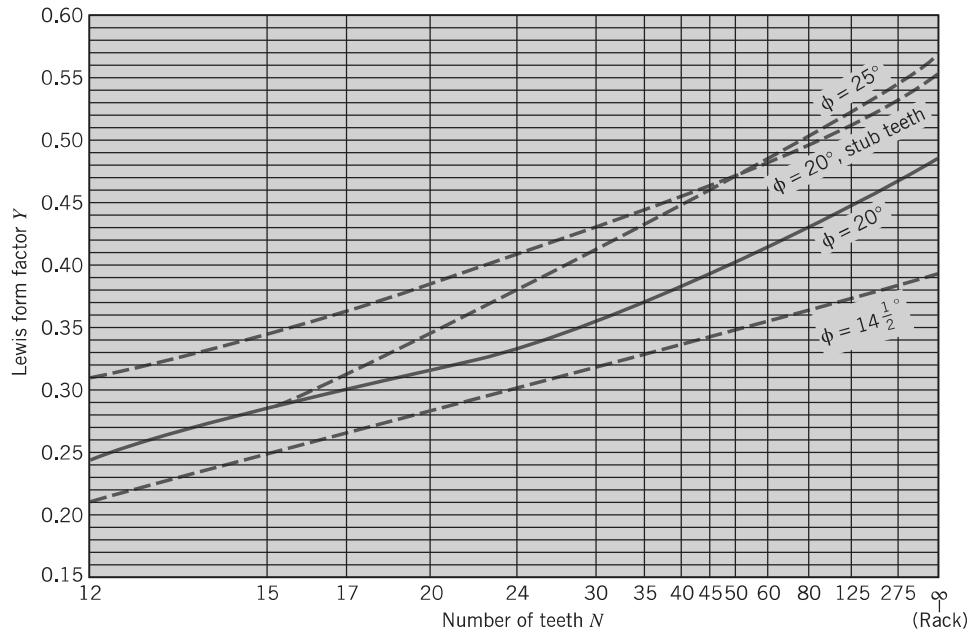


FIGURE 15.21 Values of Lewis form factor Y for standard spur gears (load applied at tip of the tooth).

Note that the Lewis equation indicates that tooth-bending stresses vary (1) directly with load F_t , (2) inversely with tooth width b , (3) inversely with tooth size p , $1/P$, or m , and (4) inversely with tooth shape factor Y or y .

15.7 Refined Analysis of Gear-Tooth-Bending Strength: Basic Concepts

In addition to the four basic factors included in the Lewis equation, modern gear design procedures take into account several additional factors that influence gear-tooth-bending stresses.

- 1. Pitch line velocity.** The greater the linear velocity of the gear teeth (as measured at the pitch circles), the greater the impact of successive teeth as they come into contact. These impacts happen because the tooth profiles can never be made with *absolute* perfection; and even if they were, deflections are inevitable, for operating loads cause a slight impact as each new pair of teeth come into engagement.
- 2. Manufacturing accuracy.** This is also an important factor influencing impact loading. Furthermore, manufacturing accuracy is the factor determining whether or not teeth do in fact share the load when two or more pairs of teeth are *theoretically* in contact. (See the first assumption in Section 15.6.)
- 3. Contact ratio.** For *precision* gears of “one-plus” contact ratio ($1 < CR < 2$), the transmitted load is divided among two pairs of teeth whenever a new tooth comes into contact at its tip. As the contact point moves down the face of the new tooth, the meshing teeth ahead

go out of contact at the highest point of single-tooth contact of the new tooth. Thus, there are two loading conditions to be considered: (a) carrying part of the load (often assumed to be half) at the tooth tip and (b) carrying the full load at the point of highest single-tooth contact. For gears of “two-plus” contact ratio ($2 < CR < 3$), we should consider a three-way division of load at tooth tip contact, and a two-way division at the highest point of double-tooth contact.

4. *Stress concentration* at the base of the tooth, as mentioned in assumption 5 of Section 15.6.
5. *Degree of shock loading* involved in the application. (This is similar to the “application factor” given for ball bearings in Section 14.7.4.)
6. *Accuracy and rigidity of mounting.* (See assumption 3, Section 15.6.)
7. *Moment of inertia of the gears and attached rotating members.* Slight tooth inaccuracies tend to cause momentary angular accelerations and decelerations of the rotating members. If the rotating inertias are small, the members easily accelerate without imposing high momentary tooth loads. With large inertias, the rotating members tend strongly to resist acceleration, thereby causing large momentary tooth loads. Significant torsional elasticity between the gear teeth and the major sources of inertia may tend to isolate the gear teeth from the harmful inertial effect. (This situation sometimes provides a fruitful area for dynamic analysis.)

The problem of gear-tooth-bending fatigue requires an evaluation of (a) the fluctuating stresses in the tooth fillet and (b) the fatigue strength of the material *at this same highly localized location*. So far only stresses have been considered; now consider the strength aspect of the problem.

The important strength property is usually the bending fatigue strength, as represented by the endurance limit. From Eq. 8.1

$$S_n = S'_n C_L C_G C_S C_T C_R$$

which, for steel members, is usually

$$S = (0.5S_u)C_L C_G C_S C_T C_R$$

Most gear teeth are loaded in *only one direction*. However, the teeth of idler gears (Figures 15.18 and 15.22a) and planet pinions (Figure 15.30, and described in Section 15.13) are loaded in both directions. Although ideally we might prefer to make a mean stress–alternating stress diagram for each particular case, reference to Figure 15.22b shows the basis for the common generalization:

For infinite life, peak stresses must be below the reversed bending endurance limit for an idler gear, but peak stresses can be 40% higher for a driving or driven gear.

For a reliability of other than 50%, gear-bending strength calculations are commonly based on the assumption that the tooth-bending fatigue strength has a normal distribution (recall Figures 6.18 through 6.20) with one standard deviation being about 8% of the nominal endurance limit.

If gear teeth operate at elevated temperatures, the fatigue properties of the material at the temperatures involved must be used.

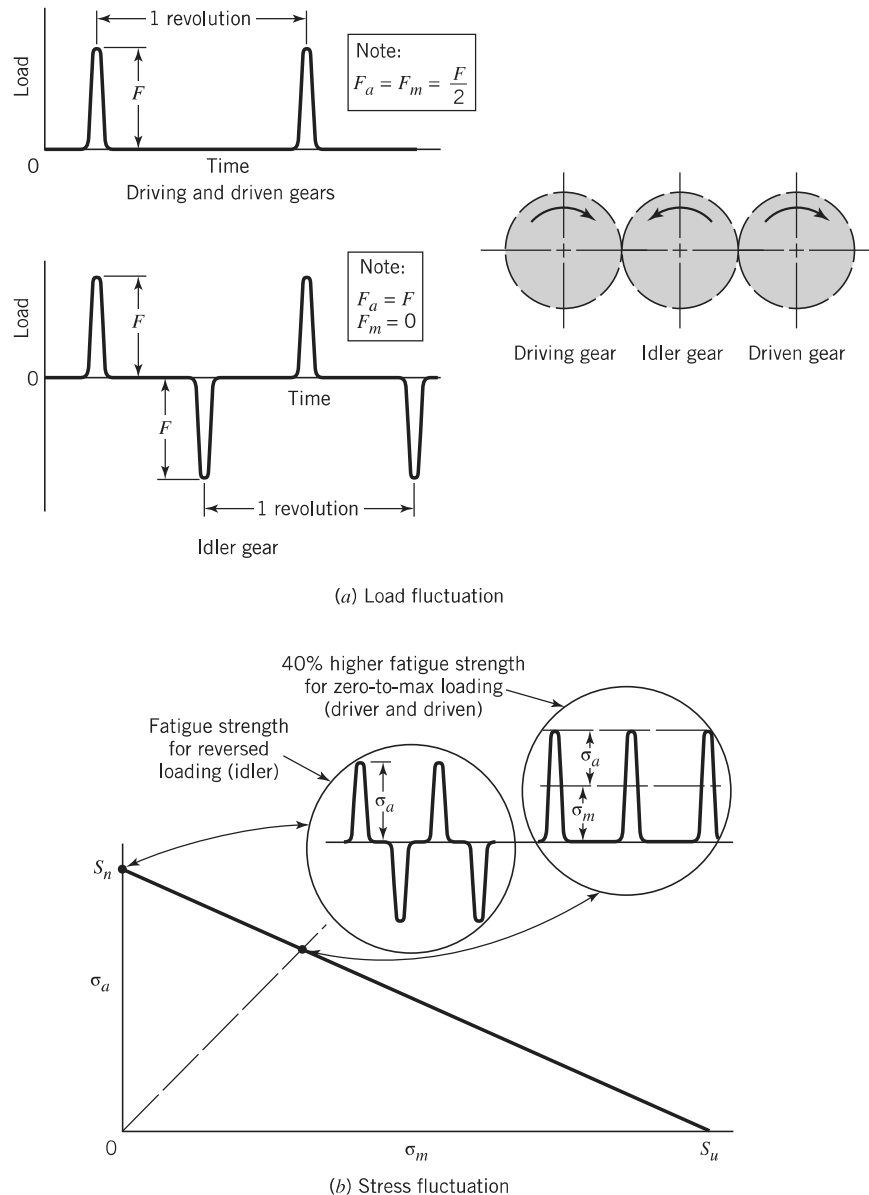


FIGURE 15.22 Load and stress fluctuations in driving, driven, and idler gears.

15.8 Refined Analysis of Gear-Tooth-Bending Strength: Recommended Procedure

The engineer seriously concerned with gear design and analysis should consult the latest standards of the American Gear Manufacturers Association and the relevant current literature. The procedures given here are representative of current practice.

In the absence of more specific information, the factors affecting gear-tooth-bending stress can be taken into account by embellishing the Lewis equation to the following form,

$$\sigma = \frac{F_t P}{bJ} K_v K_o K_m \quad (15.17)$$

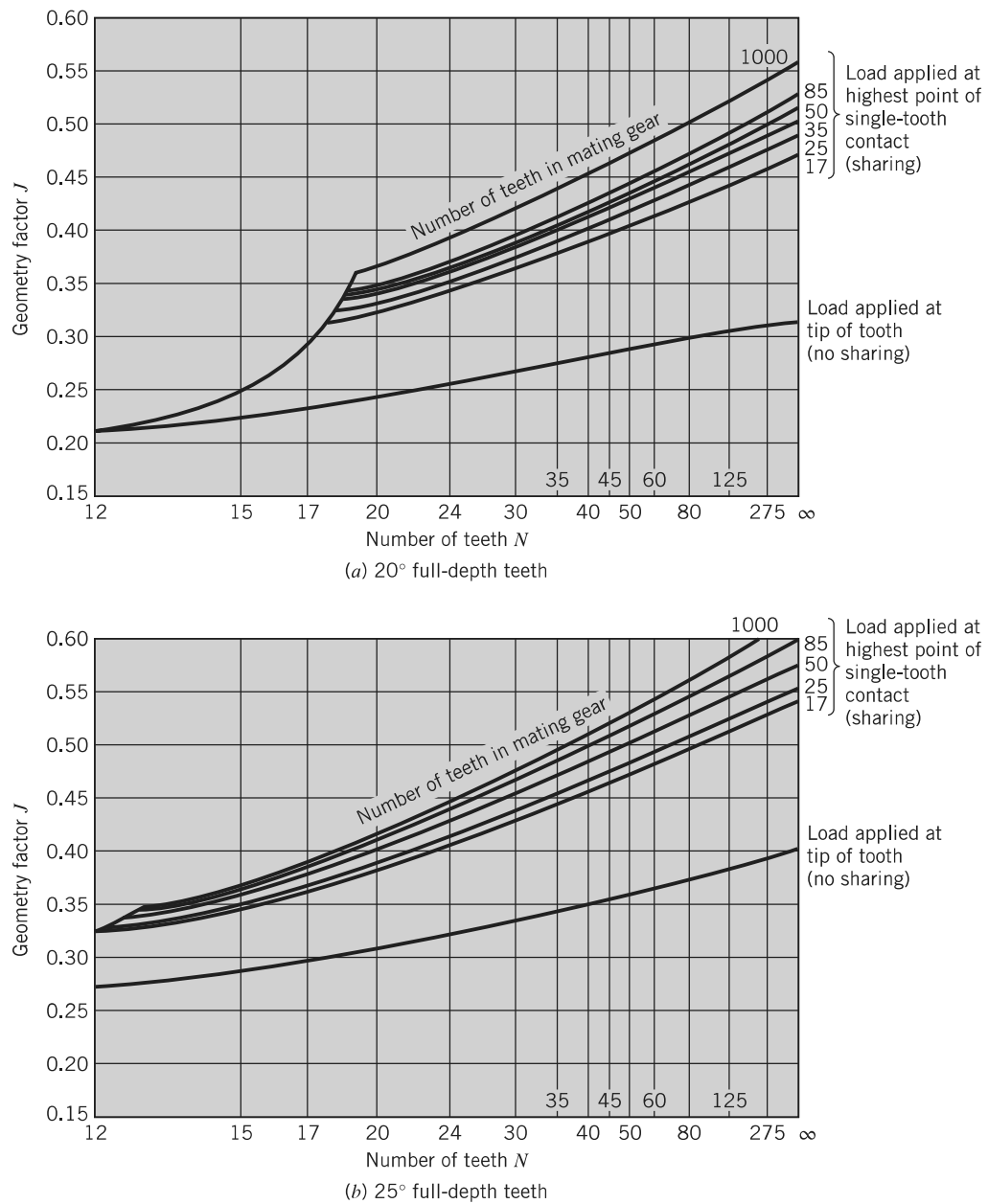


FIGURE 15.23 Geometry factor J for standard spur gears (based on tooth fillet radius of $0.35/P$). (From AGMA Information Sheet 225.01; also see AGMA 9.8-B89.)

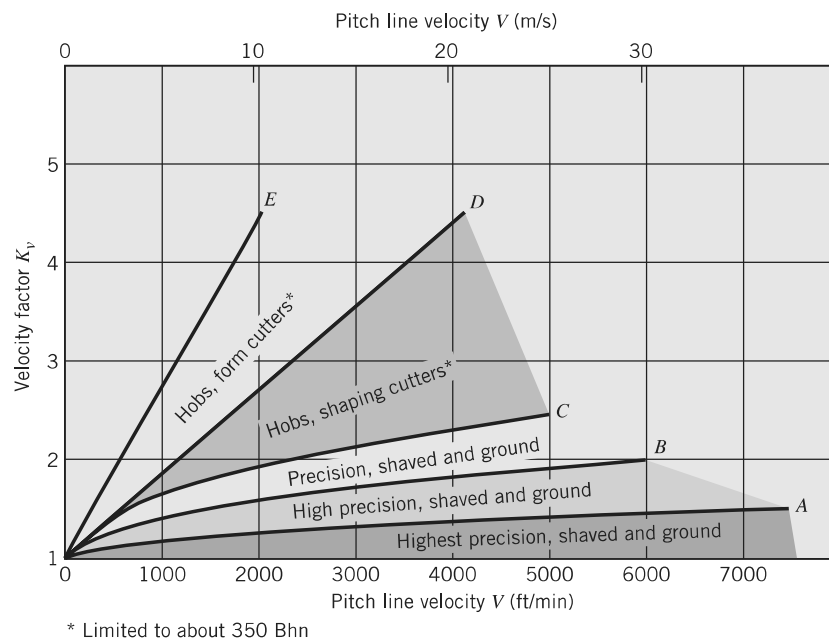
where

J = spur gear geometry factor from Figure 15.23. This factor includes the *Lewis form factor* Y and also a *stress concentration factor* based on a tooth fillet radius of $0.35/P$. Note that values are given for no load sharing (nonprecision gears) and also for load sharing (high-precision gears). In load sharing, the J factor depends on the number of teeth in the mating gear, for this controls the contact ratio, which in turn determines the highest point of single-tooth contact.

K_v = *velocity or dynamic factor*, indicating the severity of impact as successive pairs of teeth engage. This is a function of pitch line velocity and manufacturing accuracy. Figure 15.24 gives guidelines pertaining to representative gear manufacturing processes. For reference, curve A is for AGMA quality control number (class), $Q_v = 9$, curve B for $Q_v = 6$, and curve C for $Q_v = 4$ [9].

K_o = *overload factor*, reflecting the degree of nonuniformity of driving and load torques. In the absence of better information, the values in Table 15.1 have long been used as a basis for rough estimates.

K_m = *mounting factor*, reflecting the accuracy of mating gear alignment. Table 15.2 is used as a basis for rough estimates.



* Limited to about 350 Bhn

FIGURE 15.24 Velocity factor K_v . (Note: This figure, in a very rough way, is intended to account for the effects of tooth spacing and profile errors, tooth stiffness, and the velocity, inertia, and stiffness of the rotating parts.)

$$A: K_v = \sqrt{\frac{78 + \sqrt{V}}{78}} \quad D: K_v = \frac{1200 + V}{1200}$$

$$B: K_v = \frac{78 + \sqrt{V}}{78} \quad E: K_v = \frac{600 + V}{600}$$

$$C: K_v = \frac{50 + \sqrt{V}}{50}$$

Note: V is in feet per minute.

Table 15.1 Overload Correction Factor K_o

Source of Power	Driven Machinery		
	Uniform	Moderate Shock	Heavy Shock
Uniform	1.00	1.25	1.75
Light shock	1.25	1.50	2.00
Medium shock	1.50	1.75	2.25

Table 15.2 Mounting Correction Factor K_m

Characteristics of Support	Face Width (in.)			
	0 to 2	6	9	16 up
Accurate mountings, small bearing clearances, minimum deflection, precision gears	1.3	1.4	1.5	1.8
Less rigid mountings, less accurate gears, contact across the full face	1.6	1.7	1.8	2.2
Accuracy and mounting such that less than full-face contact exists	Over 2.2			

The effective fatigue stress from Eq. 15.17 must be compared with the corresponding fatigue strength. For infinite life the appropriate endurance limit is estimated from the equation

$$S_n = S'_n C_L C_G C_S k_r k_t k_{ms} \quad (15.18)$$

where

S'_n = standard R. R. Moore endurance limit

C_L = load factor = 1.0 for bending loads

C_G = gradient factor = 1.0 for $P > 5$, and 0.85 for $P \leq 5$

C_S = surface factor from Figure 8.13. Be sure that this pertains to the surface *in the fillet*, where a fatigue crack would likely start. (In the absence of specific information, assume this to be equivalent to a machined surface.)

k_r = reliability factor, C_R , determined from Figure 6.19. For convenience, values corresponding to an endurance limit standard deviation of 8% are given in Table 15.3.

k_t = temperature factor, C_T . For steel gears, use $k_t = 1.0$ if the temperature (usually estimated on the basis of lubricant temperature) is less than 160°F. If not, and in the absence of better information, use

$$k_t = \frac{620}{460 + T} \quad (\text{for } T > 160^\circ\text{F}) \quad (15.19)$$

k_{ms} = mean stress factor. In accordance with Section 15.7, use 1.0 for idler gears (subjected to two-way bending) and 1.4 for input and output gears (one-way bending).

Table 15.3 Reliability Correction Factor k_r , from Figure 6.19 with Assumed Standard Deviation of 8%

Reliability (%)	50	90	99	99.9	99.99	99.999
Factor k_r	1.000	0.897	0.814	0.753	0.702	0.659

The safety factor for bending fatigue can be taken as the ratio of fatigue strength (Eq. 15.18) to fatigue stress (Eq. 15.17). Its numerical value should be chosen in accordance with Section 6.12. Since factors K_o , K_m , and k_r have been taken into account separately, the “safety factor” need not be as large as would otherwise be necessary. Typically, a safety factor of 1.5 might be selected, together with a reliability factor corresponding to 99.9% reliability.

SAMPLE PROBLEM 15.3

Gear Horsepower Capacity for Tooth-Bending Fatigue Failure

Figure 15.25 shows a specific application of a pair of spur gears, each with face width $b = 1.25$ in. Estimate the maximum horsepower that the gears can transmit continuously with only a 1% chance of encountering tooth-bending fatigue failure.

SOLUTION

Known: A steel pinion gear with specified hardness, diametral pitch, number of teeth, face width, rotational speed, and 20° full-depth teeth drives a steel gear of 290 Bhn hardness at 860 rpm with only a 1% chance of tooth-bending fatigue failure.

Find: Determine the maximum horsepower that the gears can transmit continuously.

Schematic and Given Data:

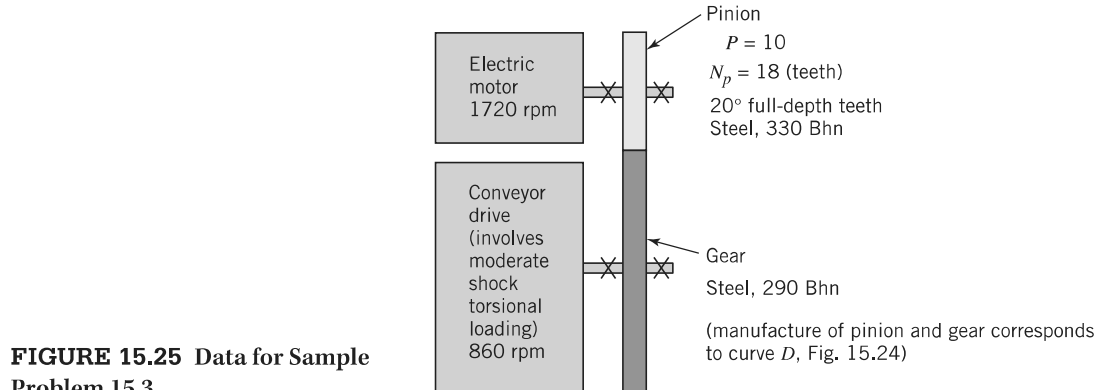


FIGURE 15.25 Data for Sample Problem 15.3.

Assumptions:

1. The gear teeth have a machined surface.
2. The gear-tooth fillet area temperature is less than 160°F.
3. The gears rotate in one direction (and hence experience one-way bending).
4. The transmitted load is applied at the tip of the gear tooth (no load sharing).
5. The manufacturing quality of the pinion and gear corresponds to curve D, Figure 15.24.

6. The output conveyor drive involves moderate torsional shock.
7. The characteristics of support include less rigid mountings, less accurate gears, and contact across the full face.
8. The gears fail solely by tooth-bending fatigue (no surface fatigue failure occurs).
9. No factor of safety will be necessary. Accounted for separately are the overload factor K_o , mounting factor K_m , and the reliability factor k_r .
10. The gears are mounted to mesh along the pitch circles.
11. The gear teeth are of equal face width.
12. The material endurance limit can be approximated by 250 (Bhn) psi.
13. The modified Lewis equation assumptions are reasonable. The J -factor data are accurate. The data plots and tables for obtaining C_a , C_s , and k_t can be relied on. The velocity factor K_v , the overload factor K_o , and the mounting factor K_m from available data are reasonably accurate.
14. The gear material is homogeneous, isotropic, and completely elastic.
15. Thermal and residual stresses are negligible.

Analysis:

1. The bending endurance strength is estimated from Eq. 15.18 as

$$S_n = S'_n C_L C_G C_S k_r k_t k_{ms}$$

where

$$\begin{aligned} S'_n &= 290/4 = 72.5 \text{ ksi (gear)} \\ &= 330/4 = 82.5 \text{ ksi (pinion)} \\ C_L &= 1 \text{ (for bending loads)} \\ C_G &= 1 \text{ (since } P > 5) \\ C_S &= 0.68 \text{ (pinion) (from Figure 8.13, machined surfaces)} \\ &= 0.70 \text{ (gear)} \\ k_r &= 0.814 \text{ (from Table 15.3; 99% reliability)} \\ k_t &= 1.0 \text{ (temperature should be } < 160^\circ\text{F)} \\ k_{ms} &= 1.4 \text{ (for one-way bending)} \\ S_n &= 63.9 \text{ ksi (pinion); } S_n = 57.8 \text{ ksi (gear)} \end{aligned}$$

2. The bending fatigue stress is estimated from Eq. 15.17 as

$$\sigma = \frac{F_i P}{b J} K_v K_o K_m$$

where

$$\begin{aligned} P &= 10 \text{ and } b = 1.25 \text{ in. (given)} \\ J &= 0.235 \text{ (pinion) (for } N = 18, \text{ no load sharing because of} \\ &\quad \text{inadequate precision of manufacture)} \\ &= 0.28 \text{ (gear) (for } N = 36, \text{ which is needed to provide the given} \\ &\quad \text{speed ratio)} \end{aligned}$$

Dynamic factor K_v involves pitch line velocity V , calculated as

$$\begin{aligned} V &= \frac{\pi d_p n_p}{12} \\ &= \frac{\pi(18 \text{ teeth}/10 \text{ teeth per inch})(1720 \text{ rpm})}{12} \\ &= 811 \text{ fpm} \end{aligned}$$

We thus have

$$K_v = 1.68 \text{ (from Figure 15.24)}$$

$$K_o = 1.25 \text{ (from Table 15.1)}$$

$$K_m = 1.6 \text{ (from Table 15.2)}$$

Therefore,

$$\sigma = 114F_t \text{ psi (pinion), } \sigma = 96F_t \text{ psi (gear)}$$

3. Equating bending fatigue strength and bending fatigue stress, we have

$$63,900 \text{ psi} = 114F_t \text{ psi, } F_t = 561 \text{ (pinion)}$$

$$57,800 \text{ psi} = 96F_t \text{ psi, } F_t = 602 \text{ (gear)}$$

4. In this case, the pinion is the weaker member, and the power that can be transmitted is (561 lb) (811 fpm) = 456,000 ft·lb/min. Dividing by 33,000 to convert to horsepower gives 13.8 hp (without provision for a safety factor).

Comments: Gear teeth generally experience several modes of failure simultaneously. Aside from tooth-bending fatigue, various other modes such as wear, scoring, pitting, and spalling may occur. These failure modes are discussed in the next section.

15.9 Gear-Tooth Surface Durability—Basic Concepts

Gear teeth are vulnerable to the various types of surface damage discussed in Chapter 9. As was the case with rolling-element bearings (Chapter 14), gear teeth are subjected to *Hertz contact stresses*, and the lubrication is often *elastohydrodynamic* (Section 13.16). Excessive loading and lubrication breakdown can cause various combinations of *abrasion*, *pitting*, and *scoring*. In this and the next section, it will become evident that gear-tooth surface durability is a more complex matter than the capacity to withstand gear-tooth-bending fatigue.

Previous sections dealt with the determination of the compressive force F acting between the gear teeth, and it was noted that the contacting surfaces are cylindrical in nature with involute profiles. Nothing has previously been said about the *rubbing velocity* of the contacting surfaces. Figure 15.26a shows the same conjugate gear teeth as in Figure 15.3, with vectors added to show velocities, V_p and V_g , of the instantaneous contact points on the pinion and gear teeth, respectively. These velocities are *tangential* with respect to their centers of rotation. If the teeth do not separate or crush together, the components of V_{pn} and V_{gn} normal to the surface must be the same. This results in their components that are tangent to the surface (V_{pt} and V_{gt}) being different. The sliding velocity is the difference between V_{pt} and V_{gt} .

Figure 15.26b shows that when contact of the mating teeth is at the *pitch point P* (i.e., on the line of centers), the sliding velocity is zero, and the tooth relative motion is one of *pure rolling*. For contact at all other points, the relative motion is one of *rolling plus sliding*, with the sliding velocity being directly proportional to the distance between the point of contact and the pitch point. The maximum sliding velocity occurs with contact at the tooth tips. This means that teeth with long addenda (as in Figure 15.8) have higher maximum sliding velocities than do corresponding gears with shorter addenda. (But, of course, the gears with shorter addenda have a smaller contact ratio.)

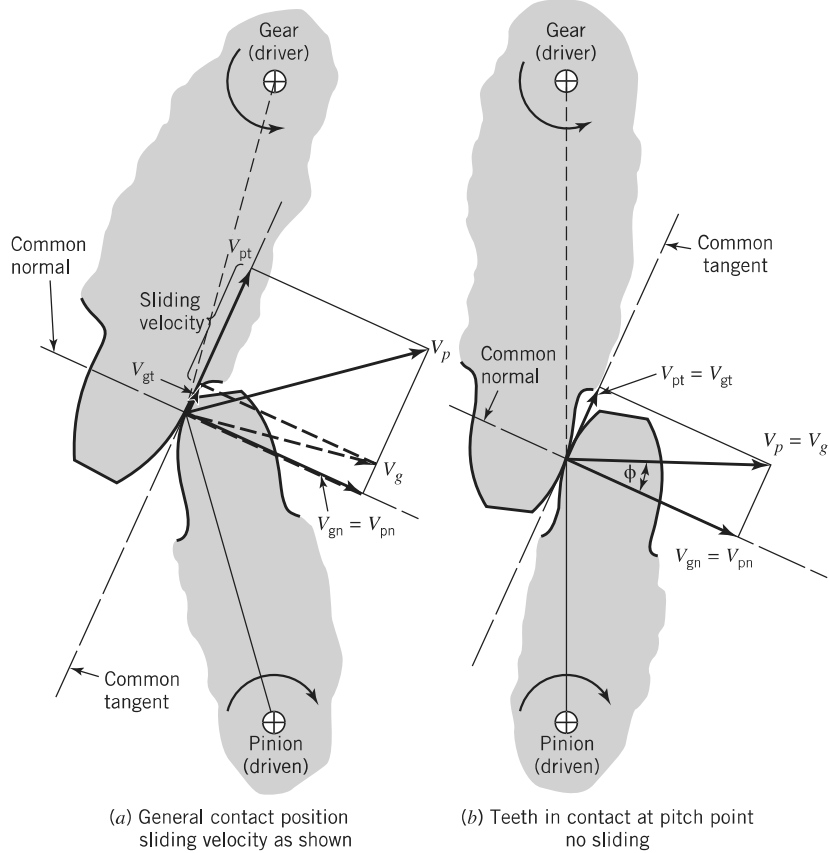


FIGURE 15.26 Gear-tooth sliding velocity.

Note that the relative sliding velocity *reverses direction* as a pair of teeth roll through the pitch point. During approach (see “angle of approach,” Figure 15.8), the sliding friction forces tend to compress the teeth; during recess, friction forces tend to elongate the teeth. The elongated teeth tend to give smoother action. For this reason, special teeth are sometimes designed to have most or all of the contact lying within the angle of recess (for the direction of rotation involved). Gear-tooth sliding can be readily demonstrated by spreading and extending the fingers of the two hands, meshing them as gears, and then rotating them.

We now consider briefly the three basic types of surface deterioration that occur in gear teeth.

1. **Abrasive wear** (treated in Section 9.10), caused by the presence of foreign particles, such as gears that are not enclosed, enclosed gears that were assembled with abrasive particles present, and gears lubricated by an oil supply with inadequate filtration.
2. **Scoring** (a form of adhesive wear described in Section 9.9), which occurs, usually at high speeds, when adequate lubrication is not provided by elastohydrodynamic action (Section 13.16) or, possibly in some instances, when boundary and mixed-film lubrications (Section 13.14) are inadequate. This causes a high coefficient of sliding friction that, together with high tooth loading and high sliding velocities, produces a high rate of heat generation in the *localized* regions of contact. This results in temperatures and pressures that cause welding and tearing apart. Scoring can often be prevented by directing an *adequate flow* (to provide cooling) of *appropriate* lubricant to the teeth as they come into mesh. An appropriate lubricant is generally one sufficiently resistant to extreme pressures

that it maintains hydrodynamic lubrication. Surface finish is also important, with finishes as fine as 20 microinches being desirable where scoring is a factor. Allowing the gears to smooth themselves during an initial “break-in” period of moderate load will increase their resistance to scoring.

3. *Pitting and spalling*, which are, respectively, surface and subsurface fatigue failures brought about by the complex stresses within the contact zone. These failures are discussed in Section 9.14.

With proper care, gears should not fail because of abrasive wear. With proper lubrication and cooling, they will not fail because of scoring. If the best heat transfer available can be provided, but an adequate lubricant cannot be found, then loads and speeds must be reduced, more score-resistant materials used, or the gears made larger. Unlike scoring, which is not time-dependent and occurs early in the operating life if at all, pitting is typical of fatigue failures because it occurs only after accumulating a sufficient number of load cycles. Furthermore, since contact stress $S-N$ curves do not level off after 10^6 or 10^7 cycles even with steel members, this type of potential surface failure must be considered in every gear design.

Generally good correlation has been observed between spur gear surface fatigue failure and the computed elastic surface stress (Hertz stress). Just as the Lewis equation serves as the basis for analyzing gear-tooth-bending strength, the Hertz stress (Eq. 9.5) is the basis for analyzing gear-tooth surface durability.

The classic work of adapting the Hertz equation to spur gear teeth was done by Earle Buckingham [1]. Buckingham noted that gear-tooth pitting occurs predominantly in the vicinity of the pitch line where, because of zero sliding velocity, the oil film (elastohydrodynamic) breaks down. Hence, he treated a pair of gear teeth as two cylinders of radii equal to the radii of curvature of the mating involutes at the pitch point. From basic involute geometry, these radii are

$$R_p = (d_p \sin \phi)/2 \quad \text{and} \quad R_g = (d_g \sin \phi)/2 \quad (15.20)$$

(Refer to Figure 15.7 and imagine the belt to be cut at P for generating the involutes.)

To adapt Eq. 9.5 (and Eq. 9.2) for convenient use with spur gears, we make the following substitutions.

Eq. 9.5 Quantity	Equivalent Notation for Spur Gears
F	F (which is equal to $F_t/\cos \phi$)
p_0	σ_H
L	b
R_1	$(d_p \sin \phi)/2$
R_2	$(d_g \sin \phi)/2$

This gives for surface (Hertz) fatigue stress

$$\sigma_H = 0.564 \sqrt{\frac{F_t[2/(d_p \sin \phi) + 2/(d_g \sin \phi)]}{b \cos \phi \left(\frac{1 - v_p^2}{E_p} + \frac{1 - v_g^2}{E_g} \right)}} \quad (15.21)$$

where b is the gear face width.

Several fundamental relationships are evident from this equation. Because of the increased contact area with load, stress increases only as the square root of load F_t (or square root of load per inch of face width, F_t/b). Similarly, contact area increases (and stress decreases) with decreased moduli of elasticity, E_p and E_g . Moreover, larger gears have greater radii of curvature, hence lower stress.

In much the same way as tooth-bending stresses, contact stresses are influenced by manufacturing accuracy, pitch line velocity, shock loading, shaft misalignment and deflection, and moment of inertia and torsional elasticity of the connected rotating members. Similarly, surface fatigue strength of the material is affected by the reliability requirement and by possible temperature extremes.

15.10 Gear-Tooth Surface Fatigue Analysis—Recommended Procedure

Equation 15.21 becomes more manageable when we (1) combine terms relating to the elastic properties of the materials into a single factor, C_p , commonly called the *elastic coefficient* and (2) combine terms relating to tooth shape into a second factor, I , commonly called the *geometry factor*:

$$C_p = 0.564 \sqrt{\frac{1}{\frac{1 - v_p^2}{E_p} + \frac{1 - v_g^2}{E_g}}} \quad (15.22)$$

$$I = \frac{\sin \phi \cos \phi}{2} \frac{R}{R + 1} \quad (15.23)$$

Here R is the ratio of gear and pinion diameters,

$$R = \frac{d_g}{d_p} \quad (\text{h})$$

Note that R is positive for a pair of external gears (Figure 15.2). Because diameters of internal gears are considered negative, R is negative for a pinion and internal gear (Figure 15.12).

Substituting C_p and I into Eq. 15.21, and also introducing factors K_v , K_o , and K_m , which were used with the bending fatigue analysis, gives

$$\sigma_H = C_p \sqrt{\frac{F_t}{bd_p I} K_v K_o K_m} \quad (15.24)$$

Note that I is a dimensionless constant that is readily calculated from Eq. 15.23, whereas C_p has units of $\sqrt{\text{ksi}}$ or $\sqrt{\text{MPa}}$, depending on the system of units used. For convenience, values of C_p are given in Tables 15.4a and 15.4b.

As noted in Sections 9.13 and 9.14, the actual stress state at the point of contact is influenced by several factors not considered in the simple Hertz equation (Eqs. 9.5, 15.21, and 15.24). These include thermal stresses, changes in pressure distribution because a lubricant is present, stresses from sliding friction, and so on. For this reason, stresses calculated from Eq. 15.24 must be compared with surface fatigue strength $S-N$ curves that have been obtained experimentally from *tests in which these additional factors were at least roughly comparable with those for the situation under study*. Thus, the surface fatigue strength curve for spur gears in Figure 9.21 is appropriate for use now, whereas the other curves in the same figure are not.

**Table 15.4a Values of Elastic Coefficient C_p for Spur Gears, in $\sqrt{\text{psi}}$
(Values Rounded Off)**

Pinion Material ($\nu = 0.30$ in All Cases)	Gear Material			
	Steel	Cast Iron	Aluminum Bronze	Tin Bronze
Steel, $E = 30,000$ ksi	2300	2000	1950	1900
Cast iron, $E = 19,000$ ksi	2000	1800	1800	1750
Aluminum bronze, $E = 17,500$ ksi	1950	1800	1750	1700
Tin bronze, $E = 16,000$ ksi	1900	1750	1700	1650

**Table 15.4b Values of Elastic Coefficient C_p for Spur Gears, in $\sqrt{\text{MPa}}$
(Values Converted from Table 15.4a)**

Pinion Material ($\nu = 0.30$ in All Cases)	Gear Material			
	Steel	Cast Iron	Aluminum Bronze	Tin Bronze
Steel, $E = 207$ GPa	191	166	162	158
Cast iron, $E = 131$ GPa	166	149	149	145
Aluminum bronze, $E = 121$ GPa	162	149	145	141
Tin bronze, $E = 110$ GPa	158	145	141	137

In the absence of information about surface fatigue strength more directly pertinent to the specific application being considered, Table 15.5 gives representative values.

As noted in Section 9.14, it is often desirable for one of the contacting members to be harder than the other. In the case of steel gears, the pinion is invariably made the harder (if they are different) because pinion teeth are subjected to a greater number of fatigue cycles and because it is generally more economical to manufacture the smaller member to the higher hardness. Typically, the hardness differential ranges from about 30 Bhn for gears in the 200-Bhn range to about 100 Bhn for the 500-Bhn range and 2 Rockwell C for the $60R_C$ range. For hardness differentials not exceeding these values, it has been found that the average hardness can be used for checking both pinion and gear.

For surface-hardened steel gears, the hardness used with Table 15.5 is the surface hardness, but the depth of the hardened case should extend down to the peak shear stresses shown in Figures 9.15b and 9.19. This would normally be at least 1 mm, or 0.040 in.

For fatigue lives other than 10^7 cycles, multiply the values of S_{fe} (from Table 15.5) by a life factor, C_{Li} , from Figure 15.27. The latter represents somewhat of an average shape of surface fatigue $S-N$ curve for steel. The alert reader will note a discrepancy between this shape (slope) and that of the $S-N$ curve for steel gears in Figure 9.21. No attempt was made to “fudge” these curves to bring them into consistency because this would mask a significant “fact of life” regarding published materials strength data. Independent studies presenting generalizations of different sets of data are likely to be at some variance and should be used with appropriate caution. If possible, it is always best to obtain good test data applying closely to the case at hand. Incidentally, the spur gear curve in Figure 9.18 is about the highest that is normally obtainable for steel gears.

Reliability data are scarce, but as a rough guide an appropriate reliability factor, C_R , as given in Table 15.6, should be used (as in Eq. 15.25).

When gear-tooth surface temperatures are high (above about 120°C , or 250°F), we must determine the appropriate surface fatigue strength for the material and temperature of the gear teeth. (A temperature correction factor for surface fatigue strength has not been included in Eq. 15.25.)

**Table 15.5 Surface Fatigue Strength S_{fe} , for Use with Metallic Spur Gears
(10^7 -Cycle Life, 99% Reliability, Temperature $< 250^\circ\text{F}$)**

Material	S_{fe} (ksi)	S_{fe} (MPa)
Steel	0.4 (Bhn)—10 ksi	2.8 (Bhn)—69 MPa
Nodular iron	0.95[0.4 (Bhn)—10 ksi]	0.95[2.8 (Bhn)—69 MPa]
Cast iron, grade 20	55	379
grade 30	70	482
grade 40	80	551
Tin bronze	30	207
AGMA 2C (11% tin)		
Aluminum bronze	65	448
(ASTM B 148—52) (Alloy 9C—H.T.)		

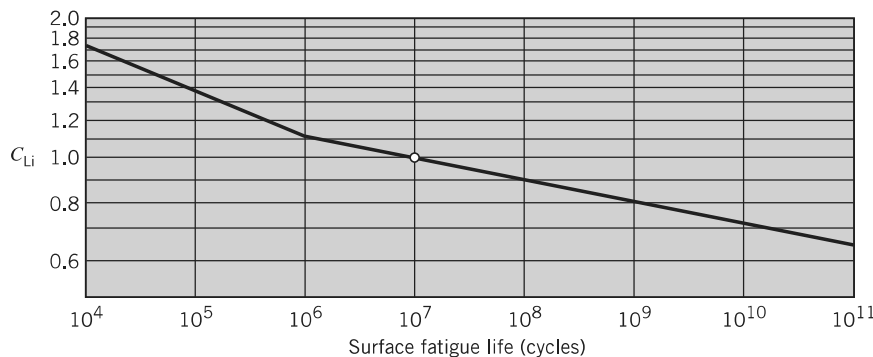


FIGURE 15.27 Values of C_{Li} for steel gears (general shape of surface fatigue $S-N$ curve).

Table 15.6 Reliability Factor C_R

Reliability (%)	C_R
50	1.25
99	1.00
99.9	0.80

Applying the information about surface fatigue strength just given, the resulting equation for gear-tooth surface fatigue strength, which should be compared to the gear-tooth surface fatigue stress from Eq. 15.24, is

$$S_H = S_{fe} C_{Li} C_R \quad (15.25)$$

In accordance with the philosophy presented in Section 6.12, the safety factor, defined as the multiplier of F_t needed to make σ_H equal to S_H , can be small. Many of the factors often included

in the “safety factor” are already taken into account by various multiplying factors in Eqs. 15.24 and 15.25. Furthermore, the consequences of failure are mitigated by the fact that pitting failures develop slowly and give warning by gradually increasing gear noise. Moreover, the extent of surface fatigue damage constituting “failure” is arbitrary, and the gears will continue to operate for some period of time after their surface endurance “life” has expired. Accordingly, safety factors of 1.1 to 1.5 are usually appropriate.

SAMPLE PROBLEM 15.4

Gear Horsepower Capacity for Tooth Surface Fatigue Failure

For the gears in Sample Problem 15.3, estimate the maximum horsepower that the gears can transmit with only a 1% chance of a surface fatigue failure during 5 years of 40 hours/week, 50 weeks/year operation.

SOLUTION

Known: The steel pinion of Sample Problem 15.3 with 330 Bhn hardness and given diametral pitch, number of teeth, rotational speed, and 20° full-depth teeth drives a steel gear of 290 Bhn at 860 rpm with only a 1% chance of surface fatigue failure during a specified time period.

Find: Estimate the maximum horsepower that the gears can transmit.

Schematic and Given Data: See Figure 15.25.

Assumptions:

1. The gear-tooth surface temperatures are below 120°C (250°F).
2. The surface fatigue endurance limit can be calculated from the surface hardness—see Table 15.5.
3. The surface fatigue stress is a maximum at the pitch point (line).
4. The manufacturing quality of the pinion and gear corresponds to curve *D*, Figure 15.24.
5. The output gear experiences moderate torsional shock.
6. The characteristics of support include less rigid mounting, less accurate gears, and contact across the full face.
7. No factor of safety will be necessary.
8. The tooth profiles of the gears are standard involutes. The contact surfaces at the pitch point can be approximated by cylinders.
9. The gears are mounted to mesh at the pitch circles.
10. The effects of surface failure from abrasive wear and scoring are eliminated by enclosure and lubrication—only pitting needs consideration.
11. The stresses caused by sliding friction can be neglected.
12. The contact pressure distribution is unaffected by the lubricant.
13. Thermal stresses and residual stresses can be neglected.
14. The gear materials are homogeneous, isotropic, and linearly elastic.
15. The surface endurance limit and life factor data available are sufficiently accurate. The velocity factor K_v , the overload factor K_o , and the mounting factor K_m obtained from available data are reasonably accurate.

Analysis:

1. The surface endurance strength is estimated from Eq. 15.25 as

$$S_H = S_{fe} C_{Li} C_R$$

where

$$S_{fe} = 114 \text{ ksi} \text{ [from Table 15.5 for steel, } S_{fe} = 0.4 \text{ (Bhn)} - 10 \text{ ksi} = 0.4(330) - 10 = 122 \text{ ksi]}$$

$$C_{Li} = 0.8 \text{ [from Figure 15.27, life} = (1720)(60)(40)(50)(5) = 1.03 \times 10^9 \text{ cycles]}$$

$$C_R = 1 \text{ (from Table 15.6 for 99% reliability)}$$

$$S_H = (122)(0.8)(1) = 97.6 \text{ ksi}$$

2. The surface (Hertz) fatigue stress is estimated from Eq. 15.24 as

$$\sigma_H = C_p \sqrt{\frac{F_t}{bd_p I} K_v K_o K_m}$$

where

$$C_p = 2300 \sqrt{\text{psi}} \text{ (from Table 15.4)}$$

$$b = 1.25 \text{ in., } d_p = 1.8 \text{ in., } K_v = 1.68, K_o = 1.25, \text{ and}$$

$$K_m = 1.6 \text{ (all are the same as in Sample Problem 15.3)}$$

$$I = \frac{\sin \phi \cos \phi}{2} \frac{R}{R+1} = 0.107 \text{ (from Eq. 15.23)}$$

$$\sigma_H = 2300 \sqrt{\frac{F_t}{(1.25)(1.8)(0.107)}} (1.68)(1.25)(1.6) = 8592 \sqrt{F_t}$$

3. Equating surface fatigue strength and surface fatigue stress gives

$$8592 \sqrt{F_t} = 97,600 \text{ psi} \quad \text{or} \quad F_t = 129 \text{ lb}$$

(This value applies to both of the mating gear-tooth surfaces.)

4. The corresponding power is $\dot{W} = F_t V = (129 \text{ lb})(811 \text{ fpm}) = 104,620 \text{ ft} \cdot \text{lb/min, or } 3.2 \text{ hp.}$

Comment: This power compares with a bending fatigue-limited power of nearly 14 hp and illustrates the usual situation of steel gears being stronger in bending fatigue. Although much of the 14-hp bending fatigue capacity is obviously wasted, a moderate excess of bending capacity is desirable because bending fatigue failures are sudden and total, whereas surface failures are gradual and cause increasing noise levels to warn of gear deterioration.

15.11 Spur Gear Design Procedures

Sample Problems 15.3 and 15.4 illustrated the analysis of estimated capacity of a given pair of gears. As is generally the case with machine components, it is a more challenging task to *design* a suitable (hopefully, near optimal) pair of gears for a given application. Before illustrating this procedure with a sample problem, let us make a few general observations.

1. Increasing the surface hardness of steel gears pays off handsomely in terms of surface endurance. Table 15.5 indicates that doubling the hardness *more* than doubles surface fatigue strength (allowable Hertz stress); Eq. 15.24 shows that doubling the allowable Hertz stress *quadruples* the load capacity F_t .
2. Increases in steel hardness also increase bending fatigue strength, but the increase is far less. For example, doubling the hardness will likely *not* double the basic endurance limit, S'_n (note flattening of curves in Figure 8.6). Furthermore, doubling hardness substantially reduces C_S (see Figure 8.13). An additional factor to be considered for surface-hardened gears is that

the hardened case may effectively increase surface fatigue strength, yet be too shallow to contribute much to bending fatigue strength (recall Figure 8.31 and the related discussion in Section 8.13).

3. Increasing tooth size (using a coarser pitch) increases bending strength more than surface strength. This fact, together with points 1 and 2, correlates with two observations. (a) A balance between bending and surface strengths occurs typically in the region of $P = 8$ for high-hardness steel gears (above about 500 Bhn, or $50R_C$), with coarser teeth failing in surface fatigue and finer teeth failing in bending fatigue. (b) With progressively softer steel teeth, surface fatigue becomes critical at increasingly fine pitches. Other materials have properties giving different gear-tooth strength characteristics. Further information about gear materials is given in the next section.
4. In general, the harder the gears, the more costly they are to manufacture. On the other hand, harder gears can be smaller and still do the same job. And if the gears are smaller, the housing and other associated parts may also be smaller and lighter. Furthermore, if the gears are smaller, pitch line velocities are lower, and this reduces the dynamic loading and rubbing velocities. Thus, overall cost can often be reduced by using harder gears.
5. If minimum-size gears are desired (for any given gear materials and application), it is best in general to start by choosing the minimum acceptable number of teeth for the pinion (usually 18 teeth for 20° pinions, and 12 teeth for 25° pinions), and then solving for the pitch (or module) required.

SAMPLE PROBLEM 15.5D Design of a Single Reduction Spur Gear Train

Using a standard gear system, design a pair of spur gears to connect a 100-hp, 3600-rpm motor to a 900-rpm load shaft. Shock loading from the motor and driven machine is negligible. The center distance is to be as small as reasonably possible. A life of 5 years of 2000 hours/year operation is desired, but full power will be transmitted only about 10% of the time, with half power the other 90%. Likelihood of failure during the 5 years should not exceed 10%.

SOLUTION

Known: A spur gear pair is to transmit power from a motor of known horsepower and speed to a driven machine shaft rotating at 900 rpm. Full power is transmitted 10% of the time, half power the other 90%. The likelihood of failure should not exceed 10% when the gears are operated at 2000 hours/year for 5 years. Center distance is to be as small as reasonably possible. (See Figure 15.28.)

Find: Determine the geometry of the gearset.

Schematic and Given Data:

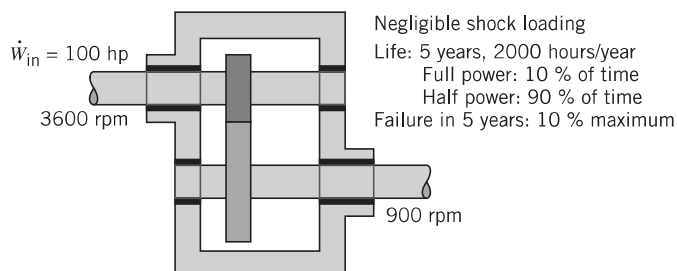


FIGURE 15.28 Single-reduction spur gear train.

Decisions:

1. Choose hardened-steel gears corresponding to the spur gear curve in Figure 9.21, which shows a 10% probability of failure. Steel gear material will be selected to provide relatively high strength at relatively low cost. The pinion and gear will be machined and then ground. In accordance with good practice, specify a case-hardening procedure that will leave compressive residual stresses in the gear-tooth surfaces.
2. Specify high surface hardness of 660 Bhn and 600 Bhn, respectively, for pinion and gear to obtain the minimum center distance and the pinion-tooth hardness that will exceed the gear-tooth hardness by 10%.
3. For these hardnesses (which are too hard for normal machining), specify a ground finish and precision manufacture corresponding to the average of curves A and B in Figure 15.24.
4. Choose the more common 20° full-depth involute tooth form.
5. Choose 18 teeth, the minimum number of pinion teeth possible to avoid interference.
6. For minimum center distance (i.e., minimum gear diameters), tentatively choose width b at the maximum of the normal range, $14/P$.
7. Choose a safety factor of 1.25 for failure by surface fatigue.
8. A nominal value for face width will be used.
9. A standard diametral pitch will be selected.

Assumptions:

1. The Palmgren–Miner cumulative-damage rule applies.
2. The ground-surface finish will correspond to the average of curves A and B in Figure 15.24, and $K_v = 1.4$.
3. The characteristics of support are accurate mountings, small bearing clearances, minimum deflection, and precision gears.
4. The spur gear curve in Figure 9.21 represents about the highest contact strength that is obtainable for steel gears, and this curve is a plot of $S_H = S_{fe} C_{Li} C_R$ for a 10% probability of failure versus the number of cycles constituting the life of the spur gear.
5. There is no load sharing between gear teeth.
6. In the limiting case, the fatigue strength of the core material must be equal to the bending fatigue stresses at the surface. Under the surface C_s is 1.
7. For the steel core material, $S'_n = 250$ (Bhn).

Design Analysis:

1. Total life required = $3600 \text{ rev/min} \times 60 \text{ min/h} \times 2000 \text{ h/yr} \times 5 \text{ yr} = 2.16 \times 10^9$ revolutions of the pinion. Only 2.16×10^8 cycles are at full power. Looking at the spur gear curve in Figure 9.21, we note that if the stresses for 2×10^8 cycles of full power are on the curve, stresses for 50% power would correspond to over 10^{10} -cycle life. Considering the Palmgren–Miner cumulative-damage rule (Section 8.12), and recognizing the approximate nature of our solution, we appear justified in designing for the full-load cycles only and in ignoring the half-load cycles.
2. Anticipating that surface fatigue will likely be more critical than bending fatigue, we solve for the value of P that will balance σ_H and S_H with a small safety factor, SF , of say 1.25:

$$\sigma_H \text{ (from Eq. 15.24)} = S_H \text{ (from Eq. 15.25)}$$

$$C_p \sqrt{\frac{F_t(SF)}{bd_p I}} K_v K_o K_m = S_{fe} C_{Li} C_R$$

A few auxiliary calculations are required:

$$V = \pi d_p (3600 \text{ rpm}) / 12 = 942d_p = 942(18/P) = 16,960/P$$

$K_v \approx 1.4$ (This value is a rough estimate from Figure 15.24,

and must be confirmed or modified after P is determined.)

$$K_m = 1.3 \text{ (This value must be increased if } b > 2 \text{ in.)}$$

$$F_t = 100 \text{ hp} (33,000)/V = 195P$$

$$I = [(\sin 20^\circ \cos 20^\circ)/2](4/5) = 0.128$$

$$S_{fe} C_{Li} C_R = 165,000 \text{ psi (directly from Figure 9.21)}$$

Substituting gives

$$2300 \sqrt{\frac{(195P)(1.25)}{(14/P)(18/P)(0.128)}}(1.4)(1)(1.3) = 165,000$$

from which

$$P = 7.21 \text{ teeth/in.}$$

3. Tentatively choose a standard pitch of 7, compute the corresponding value of V , refine the estimate of K_v , and compute the value of b required to balance σ_H and S_H . (Note that if $P = 8$ were chosen, b would have to exceed $14/P$ to balance σ_H and S_H .)

$$V = \frac{\pi d_p n_p}{12} = \frac{\pi(18/7)(3600)}{12} = 2424 \text{ fpm}$$

From Figure 15.24, $K_v = 1.5$, and

$$2300 \sqrt{\frac{(195 \times 7)(1.25)}{b(18/7)(0.128)}}(1.5)(1)(1.3) = 165,000$$

from which $b = 1.96$ in. Round off to $b = 2$ in. For this value of b , $K_m = 1.3$ is satisfactory. Also note that b remained at $14/P$ because decreasing P from 7.21 to 7 offsets increasing K_v from 1.4 to 1.5.

4. Check the contact ratio, using Eq. 15.9.

The pitch radii are $r_p = 9/7$ and $r_g = 36/7$.

The addendum, $a = 1/P$; and hence, $r_{ap} = 10/7$, $r_{ag} = 37/7$.

Center distance, $c = r_p + r_g = 45/7$.

From Eq. 15.11, $r_{bp} = (9/7) \cos 20^\circ$, $r_{bg} = (36/7) \cos 20^\circ$.

From Eq. 15.10, $p_b = \pi(18/7) (\cos 20^\circ)/18 = 0.422$ in.

Substituting in Eq. 15.9 gives CR = 1.67.

This is satisfactory, but it means that a single pair of teeth carries the load in the vicinity of the pitch line, where pitting is most likely to occur. Thus, there can be no sharing of the surface fatigue load, regardless of manufacturing precision. (Note that no sharing was assumed in the preceding calculations.)

5. We need to design the gears to provide adequate bending fatigue strength. Detailed consideration of gear-tooth-bending fatigue for case-hardened gears must include an analysis of stress and strength gradients, as represented in Figure 8.29. Since we anticipate no problem in satisfying this requirement, let us, as previously stated, make the conservative assumption that the fatigue strength of the *core* material (Eq. 15.18) must be equal to the bending fatigue stresses at the surface (Eq. 15.17):

$$S'_n C_L C_G C_S k_r k_t k_{ms} = \frac{F_t P}{b J} K_v K_o K_m$$

The manufacturing accuracy is in a “gray area” with respect to load sharing. There will likely be at least a partial sharing, meriting a value of J at least intermediate between the “sharing” and “not sharing” curves (i.e., between $J = 0.235$ and 0.32). But since we conservatively assumed no sharing, there is no need to consider the matter further. In calculating a value for C_s , remember that we are considering fatigue strength *under* the surface, where surface roughness would not be involved:

$$S'_n (1)(1)(1)(0.897)(1)(1.4) = \frac{1365(7)}{2(0.235)} (1.5)(1)(1.3)$$

From this equation $S'_n = 31,600$ psi, which requires a (core) hardness of 126 Bhn, a value that will be satisfied or exceeded by any steel selected to meet the case-hardened surface requirement.

6. In summary, our tentatively proposed design has 20° full-depth teeth, precision-manufactured with ground finish (between curves A and B of Figure 15.24) from case-hardening steel, surface-hardened to 660 Bhn and 600 Bhn, respectively, for pinion and gear, and with core hardness of at least 126 Bhn. The design also has $P = 7$, $N_p = 18$, $N_g = 72$, $b = 2$ in. ($D_p = 2.57$ in., $D_g = 10.29$ in., $c = 6.43$ in.). As decided, we will specify a case-hardening procedure leaving compressive residual stresses in the surfaces.

Comment: This sample problem represents but one of a great many situations and approaches encountered in the practical design of spur gears. The important thing for the student is to gain a clear understanding of the basic concepts and to understand how these may be brought to bear in handling specific situations. We have seen that a great amount of empirical data is needed in addition to the fundamentals. It is always important to seek out the best and most directly relevant empirical data for use in any given situation. Textbooks such as this can include only sample empirical information. Better values for actual use are often found in company files, contemporary specialized technical literature, and current publications of the AGMA.

15.12 Gear Materials

The least expensive gear material is usually ordinary cast iron, ASTM (or AGMA) grade 20. Grades 30, 40, 50, and 60 are progressively stronger and more expensive. Cast-iron gears typically have greater surface fatigue strength than bending fatigue strength. Their internal damping tends to make them quieter than steel gears. Nodular cast-iron gears have substantially greater bending strength, together with good surface durability. A good combination is often a steel pinion mated to a cast-iron gear.

Steel gears that have not been heat-treated are relatively inexpensive but have low surface endurance capacity. Heat-treated steel gears must be designed to resist warpage; hence, alloy steels and oil quenching are usually preferred. For hardnesses of more than 250 to 350 Bhn, machining must usually be done before hardening. Greater profile accuracy is obtained if the surfaces are finished after heat treating, as by grinding. (But if grinding is done, care must be taken to avoid residual tensile stresses at the surface.) Through-hardened gears generally have 0.35 to 0.6% carbon. Surface- or case-hardened gears are usually processed by flame hardening, induction hardening, carburizing, or nitriding.

Of the nonferrous metals, bronzes are most often used for making gears.

Nonmetallic gears made of acetal, nylon, and other plastics are generally quiet, durable, reasonably priced, and can often operate under light loads without lubrication. Their teeth deflect more easily than those of corresponding metal gears. This promotes effective load sharing among teeth in simultaneous contact but results in substantial hysteresis heating if the gears are rotating at high speed. Since nonmetallic materials have low thermal conductivity, special cooling provisions may be required. Furthermore, these materials have relatively high coefficients of thermal expansion, and thus, they may require installation with greater backlash than metal gears.

Often, the base plastics used for gears are formulated with fillers, such as glass fibers, for strength, and with lubricants such as Teflon for reduced friction and wear. Nonmetallic gears are usually mated with cast iron or steel pinions. For best wear resistance, the hardness of the mating metal pinion should be at least 300 Bhn. Design procedures for gears made of plastics are similar to those for gears made of metals, but are not yet as reliable. Hence, prototype testing is even more important than for metal gears.

15.13 Gear Trains

The speed ratio (or “gear ratio”) of a single pair of *external* spur gears is expressed by the simple equation

$$\frac{\omega_p}{\omega_g} = \frac{n_p}{n_g} = -\frac{d_g}{d_p} = -\frac{N_g}{N_p} \quad (15.26)$$

(an expanded version of Eq. 15.1) where ω and n are rotating speed in radians per second and rpm, respectively, d represents pitch diameter, and N is the number of teeth. The minus sign indicates that an ordinary pinion and gear (both with external teeth) rotate in *opposite* directions. If the gear has internal teeth (as in Figure 15.12), its diameter is negative and the members rotate in the *same* direction. In most applications, the pinion is the driver and the gear the driven, which provides a *reduction ratio* (reduction in speed, but increase in torque). This is so because power sources (engines, motors, and turbines) usually rotate relatively fast in order to provide a large amount of power from a given size unit. The machinery being driven usually runs slower. (There are exceptions, for example, engine-driven superchargers and large centrifugal compressors for refrigeration and air conditioning.)

Figure 15.29 shows a double-reduction gear train involving countershaft b as well as input shaft a and output shaft c . The overall speed ratio is

$$\begin{aligned} \frac{\omega_a}{\omega_c} &= \frac{\omega_a \omega_b}{\omega_b \omega_c} = -\frac{d_{g1}}{d_{p1}} \left(-\frac{d_{g2}}{d_{p2}} \right) \\ &= +\frac{d_{g1} d_{g2}}{d_{p1} d_{p2}} = \frac{N_{g1} N_{g2}}{N_{p1} N_{p2}} \end{aligned} \quad (15.27)$$

Note that if the two gear pairs have the same center distance, the input and output shafts can be in exact alignment, which may facilitate economical manufacture of the housing.

Figure 15.29 and Eq. 15.27 can be extended to three, four, or any number of gear pairs, with the overall ratio being the product of the ratios of the individual pairs. Familiar examples are the gear trains in odometers and in mechanical watches and clocks.

Planetary (or *epicyclic*) gear trains are more complicated to analyze because some of the gears rotate about axes that are *themselves* rotating. Figure 15.30a illustrates a typical planetary train, which includes a sun gear S at the center, surrounded by planets P that rotate freely on shafts mounted in arm A (also called the “carrier”). Also meshing with the planets is a ring or annulus gear R that has internal teeth. Figure 15.30b is a simplified version in that only a single planet is shown. Actual planetary trains incorporate two or more planets, equally spaced, to balance the force acting on the sun, ring, and arm. Dividing the load between multiple planets correspondingly increases the torque and power capacity of the train. When we analyze planetary train speed ratios, it may be more convenient to refer to the single-planet drawing (Figure 15.30b).

The three members S , A , and R are normally assigned three functions: input, output, and fixed reaction member. Let us examine three alternative arrangements. (1) With A as the reaction member, we have a simple gear train (all the axes are fixed), and members S and R rotate in opposite

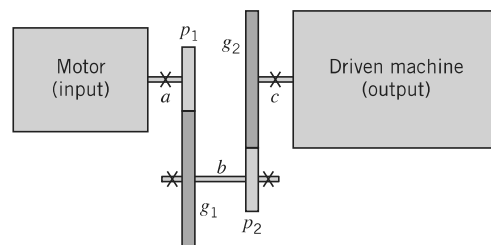


FIGURE 15.29 Double-reduction gear train.

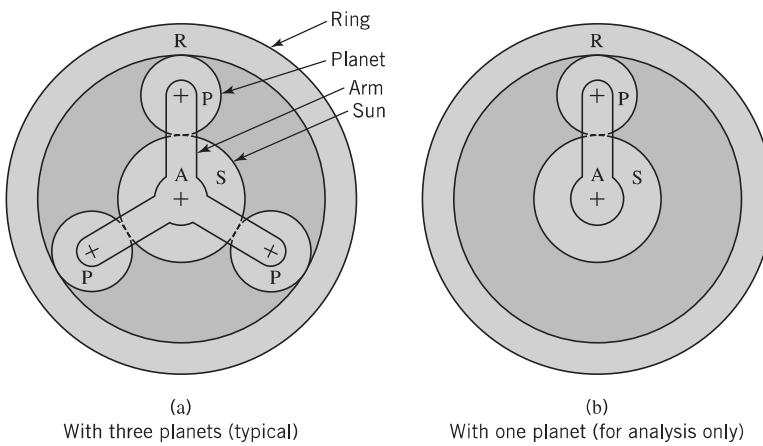


FIGURE 15.30 Typical planetary gear train.

directions, providing a reverse gear. (2) With R held fixed, S and A rotate in the same direction but at different speeds. (3) With S fixed, R and A also rotate in the same direction but with different speed ratios than when R is fixed. Regardless of the arrangement chosen, we can install a clutch enabling any two of members S , A , and R to be locked together. This causes the entire planetary train to rotate as a single member and provides a *direct drive* (gear ratio = 1) from input to output. Automotive automatic transmissions use combinations of planetary gear trains, with a clutch for direct drive and with brakes or one-way clutches to hold various members fixed to obtain the different ratios.

We now present three methods for determining planetary gear ratios, illustrated for the train shown in Figure 15.30 with R as the input, A as the output, and S as the fixed reaction member. In order to simplify the notation, letters R , S , and P represent either the diameters or the numbers of teeth in the ring, sun, and planet, respectively.

1. *Free-body force analysis.* Figure 15.31 shows an exploded diagram of three components. Using the given notation, we find the arm radius is equal to

$$\frac{S + P}{2} = \frac{S + (R/2 - S/2)}{2} = \frac{R + S}{4}$$

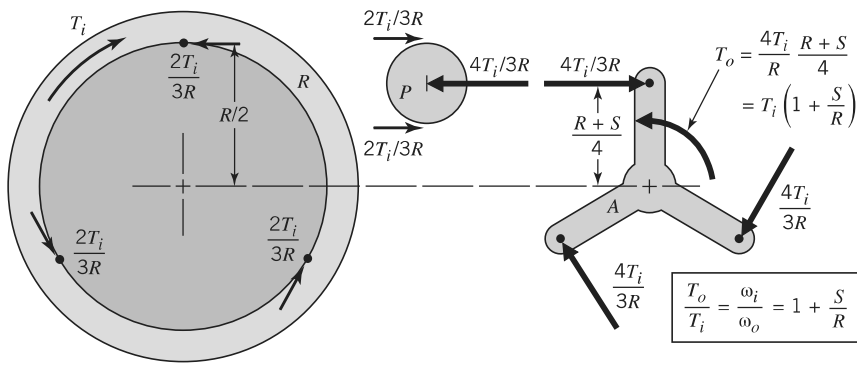


FIGURE 15.31 Torque ratio (1 divided by the speed ratio) determined by free-body diagrams.

(as shown). Starting with input torque T_i applied to the ring, we place loads on each of the members to put them in equilibrium. This leads to the conclusion that

$$\frac{\omega_i}{\omega_o} = \frac{T_o}{T_i} = 1 + \frac{S}{R} \quad (\text{i})$$

2. *Velocity vector analysis.* Figure 15.32 shows arbitrary velocity vector V drawn at the meshing of R and P . The linear velocity is zero at the meshing of S and P because the sun is fixed. Angular velocities of R and A are determined as the ratios of linear velocities to corresponding radii. This analysis again leads to Eq. i.
3. *General planetary train equation.* In Figure 15.30 (and with no member necessarily held fixed), the angular velocity of the ring with respect to the arm and of the sun with respect to the arm are, by definition,

$$\omega_{R/A} = \omega_R - \omega_A \quad \text{and} \quad \omega_{S/A} = \omega_S - \omega_A$$

from which

$$\frac{\omega_{R/A}}{\omega_{S/A}} = \frac{\omega_R - \omega_A}{\omega_S - \omega_A} \quad (\text{j})$$

Equation j is true for *any* angular velocity of the arm, including zero. With the arm fixed, angular velocity ratios are computed from Eq. 15.27, and the result is known as the *train value*, e . Thus,

$$\frac{\omega_{R/A}}{\omega_{S/A}} = \frac{\omega_R}{\omega_S} = e = \left(-\frac{S}{P} \right) \left(+\frac{P}{R} \right) = -\frac{S}{R} \quad (\text{k})$$

Combining j and k gives

$$e = -\frac{S}{R} = \frac{\omega_R - \omega_A}{\omega_S - \omega_A} \quad (15.28)$$

where R and S again represent either the pitch diameters or numbers of teeth in the ring and sun gears. Applying Eq. 15.28 to Figure 15.30 with S the fixed member, we once more obtain Eq. i.

To adapt Eq. 15.28 to a complex planetary train, first identify the three members providing the input, output, and reaction functions. One of these will be the arm. Call the other two X and Y . Then the train value is

$$e = \frac{\omega_X}{\omega_Y} = \frac{\omega_X - \omega_A}{\omega_Y - \omega_A} \quad (15.29)$$

The Figure 15.31 arrangement with S fixed is perhaps the most commonly used planetary train. Depending on the relative gear sizes, the value of the ratio determined from Eq. 15.28

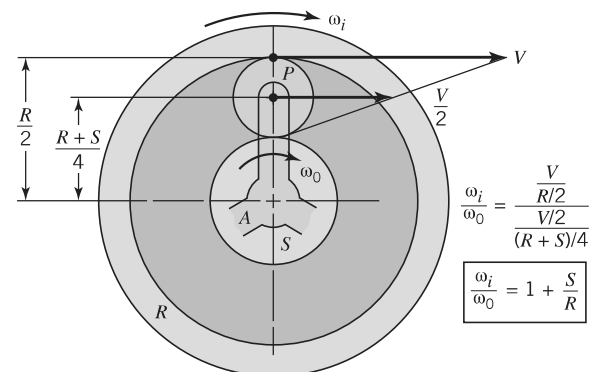


FIGURE 15.32 Speed ratio determined by velocity vector diagram.

(R = input; A = output; S = fixed member)

can be any value between 1 and 2. With R as the input and A the output, this train is often used as a reduction gear for propeller-driven aircraft. With A as the input and R the output, it is the basis of the conventional automotive overdrive. Perhaps the most familiar application of all is the Sturmey–Archer 3-speed bicycle hub, which is shifted between (1) low gear, connected as in the aircraft reduction gear, (2) intermediate gear, with all parts rotating together for direct drive, and (3) high gear, connected as in the automotive overdrive—a very ingenious arrangement—see <http://www.sturmey-archer.com>.

In Figure 15.31, it was assumed that the load is divided equally among all planets. Actually, this happens only if (1) the parts are made with sufficient precision or (2) special construction features are employed to equalize the loading automatically.

There are two basic factors that control the number and spacing of the planets employed. (1) The maximum number of planets is limited by the space available—that is, the tooth tips of any planet must clear those of the adjacent planets. (2) The teeth of each planet must align simultaneously with teeth of the sun and annulus. Figure 15.33 shows an example in which the second condition is satisfied for two equally spaced planets but not for four. (The reader is invited to continue this study and show that with the geometry and tooth numbers used in Figure 15.33, a necessary condition for the *possibility* of equidistant assembling of planet gears, n , requires that $(S + R)/n = i$, where i is an integer and n is the number of equally spaced planet gears—see [8].)

Traction drives are gaining popularity as an alternative technology to gear trains. Traction drives operate by transmitting power through rotating components separated by a microscopic layer of a special type of elastohydrodynamic fluid commonly known as traction fluid. Under

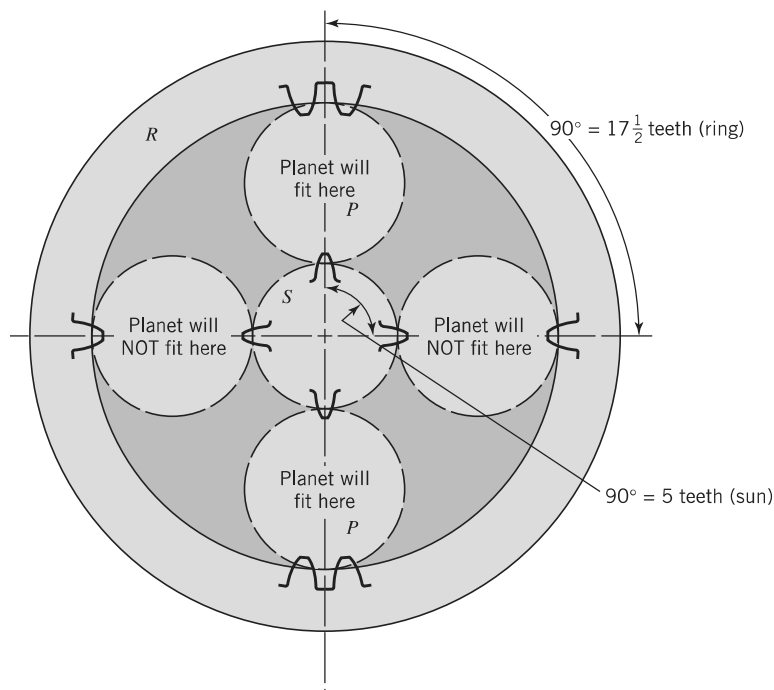


FIGURE 15.33 Geometric study of two versus four equally spaced planets for a 20-tooth sun and a 70-tooth ring.

1. Planets must have $(70 - 20)/2 = 25$ teeth. Because the number of planet gear teeth is an odd number, the sun and ring *must* be aligned with a sun tooth opposite a ring space between teeth, as shown at the top and bottom positions.
2. With sun and ring properly indexed for top and bottom planets, the two side planets will *not* fit.
3. Conclusion: Two equally spaced planets can be used; four cannot.

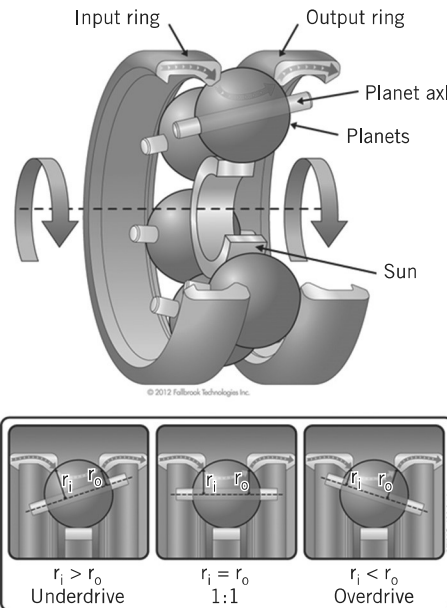


FIGURE 15.34 Fallbrook Technologies, Inc. NuVinci® continuously variable planetary traction drive. (Fallbrook Technologies Inc.)

normal conditions, this fluid is similar to transmission fluid and provides lubrication and cooling. However, traction fluid contains constituent elements that cause its viscosity to significantly increase, momentarily solidifying, as it passes through the high-pressure contact patch between the components. This feature allows the fluid to sustain high shear forces and effectively transmit power. This layer of fluid also prevents the rolling components from contacting, which reduces wear. A key benefit of traction drives is that they provide continuously variable ratio changes, avoiding the stepped ratios inherent to a gear train or geared transmission. Various configurations of traction drives have been developed, including designs utilizing toroidal rollers and various configurations utilizing rolling balls. The continuously variable planetary traction drive shown in Figure 15.34 uses a set of balls to transmit power and is analogous to a planetary gear train. Power can be input or output on the sun, carrier, or rings, and the drive can be used to sum or split power. The ratio between input speed and output speed is varied by tilting the planet axle to change the contact radii. Additional information and sample problems on traction drive technology, traction fluids, and a variety of traction drive designs can be found at www.nuvinci.com/traction-drives.

REFERENCES

1. Buckingham, Earle, *Analytical Mechanics of Gears*, McGraw-Hill, New York, 1949.
2. Dudley, D. W. (ed.), *Gear Handbook*, McGraw-Hill, New York, 1962.
3. Dudley, D. W., *Handbook of Practical Gear Design*, CRC Press, Boca Raton, FL, 1994.
4. Kelley, O. K., "Design of Planetary Gear Trains," Chapter 9 of *Design Practices—Passenger Car Automatic Transmissions*, Society of Automotive Engineers, New York, 1973.
5. "1981 Mechanical Drives Reference Issue," *Machine Design*, Penton/IPC, Cleveland, June 18, 1981.
6. Merritt, H. E., *Gear Engineering*, Pitman Publishing, Marshfield, MA, 1971.
7. Standards of the American Gear Manufacturers Association, Alexandria, VA.
8. Simionescu, P. A., "A Unified Approach to the Assembly Condition of Epicyclic Gears," *ASME J. Mech. Design*, **120**: 448–452 (1998).
9. "Fundamental Rating Factors and Calculation Methods for Involute Spur and Helical Gear Teeth," Standard ANSI/AGMA 2001-D04, American Gear Manufacturers Association, Alexandria, VA, 2004.